

CHAPTER 4

EXPERIMENTAL RESULTS

This chapter will present the results obtained from the methodologies of Chapter 3. First, the characterization data will be presented, then the water-breaking data, and finally the calibration data. Four transducers with PZT-4 spherical crystals [Boston Piezo-Optics Inc., Bellingham, MA] were used in this study. The transducers studied are named blue, orange, yellow, and red.

4.1 Characterization Data

The properties of the four transducers were determined from the characterization procedure (Section 3.1) and are listed in Table 4.1. The properties for the

Transducer	Center Frequency	Wavelength (μ m)	Beamwidth (mm)	Focal Length (mm)
blue	3.00 MHz	495	1.1	116
orange	3.32 MHz	447	1.2	135
yellow	3.03 MHz	493	2.7	291
red	2.11 MHz	706	1.7	98

Table 4.1 Characterization Results for blue, orange, yellow, and red Transducers

orange and blue transducer at their third harmonic are listed in Table 4.2. The additional

Transducer	Frequency	Wavelength (μ m)	Beamwidth (mm)
blue	9.00 MHz	164	0.37
orange	10.0 MHz	150	0.38

Table 4.2 Properties of the blue and orange Transducer at the Third Harmonic

information is used to obtain measurements at a different carrier frequency which would result in a different size beamwidth.

4.2 Water-Breaking Study Data

The purpose of the water-breaking study is to determine the ultrasonic field quantity that would just fracture the water-air boundary and the corresponding distance between the transducer and water surface. Figure 4.2 shows an image of the water-air boundary just before it is broken and Figure 3.7 shows an image of the water-air boundary just after it is broken.

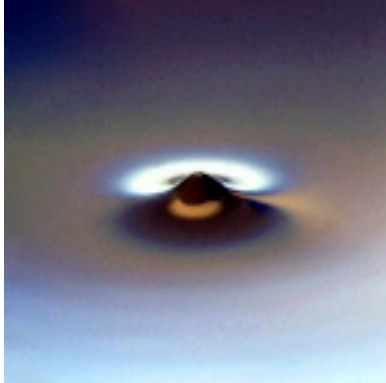


Figure 4.1 Image of the Water-Air Boundary Just Before the Boundary is Broken

Water-breaking data were taken for each of the transducers at their center frequency and at the third harmonic for the orange and blue transducers. The water-breaking study was performed under continuous and pulsed wave conditions. The study was repeated five times for each condition and frequency (Figures A.5-A.16).

The water-breaking data, which gives a range of distances between the transducer surface and the water surface along with the corresponding water-breaking voltage value for that distance (Figures A.5-A.16), were used in determining the quantities of Table 4.3. This table shows the transducer frequency and the conditions (continuous or pulsed wave) under which the water-breaking study occurred along with the minimum water-breaking voltage value required and the distance where this minimum water-breaking voltage occurred.

Color	Frequency (MHz)	Continuous/ Pulsed Wave	Water-Breaking Distance (mm)	Threshold Water-Breaking Voltage Value (mV)	
				Average	Std Dev

Blue	3.00	Continuous	135	26.5	0.25
Blue	3.00	1 kHz	139	276	3.43
Blue	3.00	500 Hz	139	349	5.25
Blue	9.0	Continuous	149	218	1.92
Blue	9.0	1 kHz	150	826	28.40
Blue	9.0	500 Hz	149	832	8.96
Orange	3.3	Continuous	146	20.6	0.65
Orange	3.3	1 kHz	149	233	1.23
Orange	3.3	500 Hz	148	364	1.87
Orange	10.0	Continuous	148	136	5.55
Orange	10.0	1 kHz	145	472	15.23
Orange	10.0	500 Hz	145	595	17.08
Red	2.1	Continuous	95	21.2	0.15
Red	2.1	1 kHz	98	105	0.17
Red	2.1	500 Hz	98	131	0.83
Yellow	3.03	Continuous	314	41.7	0.28
Yellow	3.03	11 kHz	291	151	0.59
Yellow	3.03	9 kHz	291	291	1.87

Table 4.3 Focal Lengths and Corresponding Minimum Average Water-Breaking Voltage Value With Standard Deviations for all Transducers

4.3 Calibration Data

The calibration procedure measured the peak compressional pressure, peak rarefactional pressure, and voltage intensity integral of the ultrasonic beam. As described in Section 3.2 and 3.3, the water-breaking voltage values are the settings used to calibrate the transducer. The peak compressional and peak rarefactional pressures as a function of the voltage setting were measured and plotted with their standard deviations (Figures A.17-A.28).

The peak compressional and peak rarefactional threshold water-breaking pressures for each of the transducer settings were determined. This was done by determining the minimum water-breaking voltage values, (Table 4.3) and calculating the voltage-to-pressure relationship (Figures A.17-A.28). The voltage-to-pressure equations were determined by performing a linear regression analysis. Table 4.4 shows the peak compressional and peak rarefactional pressure equations for the corresponding water-breaking voltage values from Table 4.3 at each setting.

Settings	P_c Equation	P_r Equation
Blue 3.0 MHz, CW	$P_c = 0.0775*v - 0.4729$	$P_r = 0.0409*v + 0.0398$
Blue 3.0 MHz, PRF= 1 kHz	$P_c = -0.116*v + 49.321$	$P_r = -0.00846*v + 9.0384$
Blue 3.0 MHz, PRF= 500 Hz	$P_c = -0.0225*v + 26.0168$	$P_r = 0.0210*v + 0.111$
Blue 9.0 MHz, CW	$P_c = 0.0540*v - 9.01$	$P_r = 0.0160*v - 2.221$
Blue 9.0 MHz, PRF= 1 kHz	$P_c = 0.460*v - 360.6$	$P_r = 0.370*v - 294.883$
Blue 9.0 MHz, PRF= 500 Hz	$P_c = 0.530*v - 418.667$	$P_r = 0.300*v - 237.1$
Orange 3.3 MHz, CW	$P_c = 0.126*v - 0.994$	$P_r = 0.0464*v + 0.139$
Orange 3.3 MHz, PRF= 1 kHz	$P_c = 0.0220*v + 12.477$	$P_r = 0.0612*v - 8.731$
Orange 3.3 MHz, PRF= 500 Hz	$P_c = 0.0500*v + 1.117$	$P_r = 0.0299*v - 4.283$
Orange 10 MHz, CW	$P_c = 0.0861*v - 9.827$	$P_r = 0.0259*v - 2.238$
Orange 10 MHz, PRF= 1 kHz	$P_c = 0.382*v - 160.787$	$P_r = 0.192*v - 80.863$
Orange 10 MHz, PRF= 500 Hz	$P_c = 0.431*v - 234.841$	$P_r = 0.195*v - 103.775$
Red 2.1 MHz, CW	$P_c = 0.0968*v - 0.483$	$P_r = 0.0276*v + 0.340$
Red 2.1 MHz, PRF= 1 kHz	$P_c = 0.205*v - 8.253$	$P_r = 0.0414*v + 1.163$
Red 2.1 MHz, PRF= 500 Hz	$P_c = 0.315*v - 23.143$	$P_r = 0.0836*v - 4.426$
Yellow 3.03 MHz, CW	$P_c = 0.108*v - 2.3926$	$P_r = 0.0153*v + 0.162$
Yellow 3.03 MHz, PRF= 11kHz	$P_c = 0.0204*v + 0.890$	$P_r = 0.00898*v + 0.445$
Yellow 3.03 MHz, PRF= 9kHz	$P_c = 0.00481*v + 3.304$	$P_r = -0.00103*v + 2.588$

Table 4.4 Equations for the Water-Breaking Compressional and Rarefactional Pressure, v is the Corresponding Water-Breaking Voltage Value from Table 4.3

The threshold water-breaking peak compressional and peak rarefactional pressures for each of the transducers are plotted (Figure 4.2).

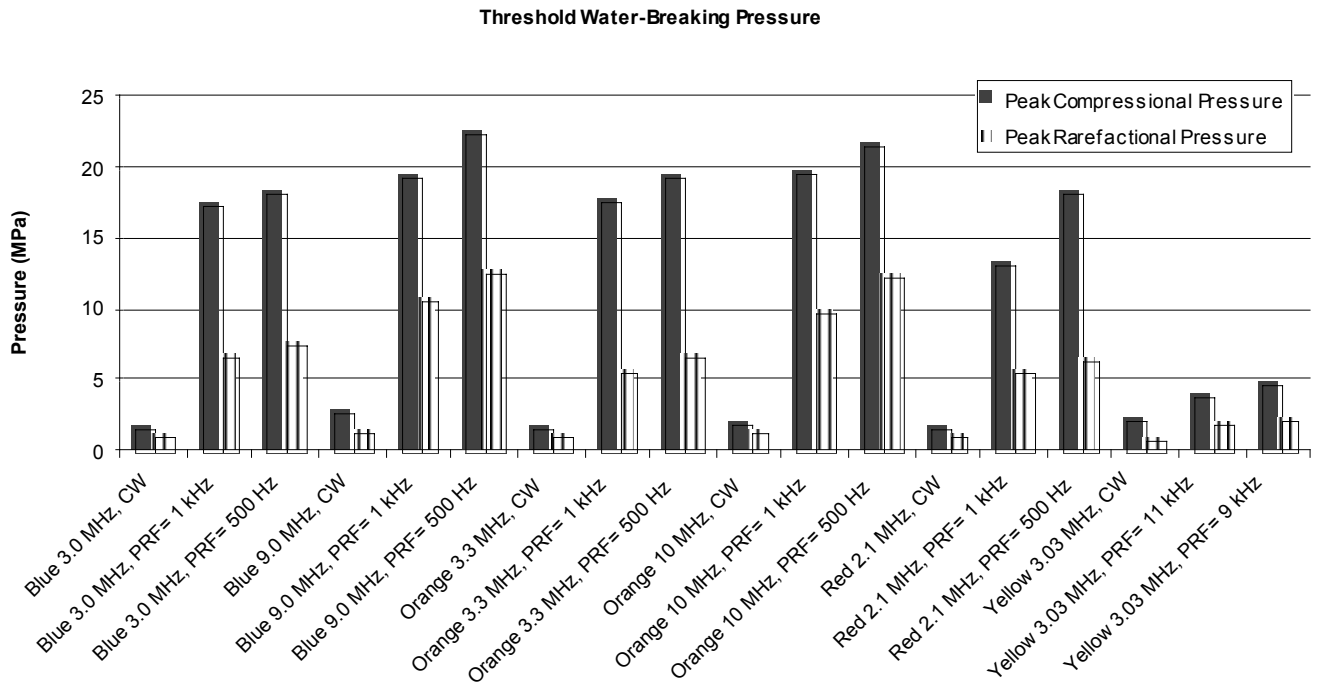


Figure 4.2 Peak Compressional and Rarefactional Threshold Water-Breaking Pressures

The overall trend (Figure 4.2) is as the pulse repetition frequency decreases, the average threshold water-breaking compressional and rarefactional pressures increase. This can be seen for all transducers.

In addition to observing how the pulse repetition frequency affects the threshold water-breaking pressure, the effects of beamwidth on water-breaking pressure were also studied.

Figures 4.3-4.7 show how the threshold water-breaking rarefactional pressure (y-axis) changes with a change in the beamwidth (x-axis). Figure 4.3 is the threshold water-breaking rarefactional pressure for the continuous wave case and Figure 4.5 is the threshold water-breaking rarefactional pressure for the pulsed case, where the pulse repetition frequency is 1 kHz. Figure 4.6 is the threshold water-breaking rarefactional pressure for the pulsed case, where the pulse repetition frequency is 500 Hz.

Figure 4.3 (continuous wave case) shows an overall decrease in the threshold water-breaking rarefactional pressure as the beamwidth increases.

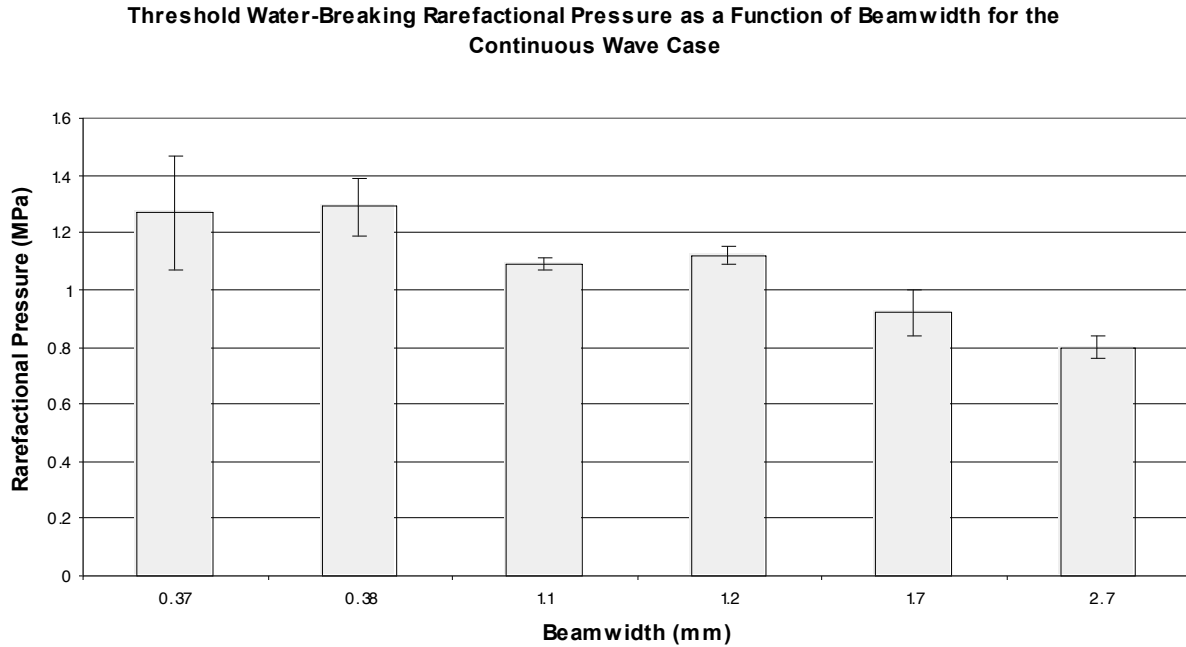


Figure 4.3 Threshold Water-Breaking Rarefactional Pressure for the Continuous Wave Case with Beamwidth Dependency

Assuming there is a linear relationship between the beamwidth and threshold water-breaking rarefactional pressure, a linear regression analysis was performed. The regression analysis provided the correlation coefficient (r^2) and a p-value which indicated the significance of the slope relative to a zero slope. The p-value helps in determining if a relationship between a set of variables exist. In this case, the relationship between beamwidth and threshold water-breaking rarefactional pressure was studied. A p-value of 0.05 was established as the level of test. If the p-value is less than or equal to 0.05, the null hypothesis is rejected. A p-value of 0.05 means that there is a 5% chance that the results could have been obtained although there was no correlation between the two variables.

Figure 4.4 shows the threshold water-breaking rarefactional pressure for the continuous wave case plotted as a function of increasing beamwidth. The regression line in Figure 4.4 has the equation $P = -0.125b + 1.349$, where P is the threshold water-breaking rarefactional pressure in MegaPascals and b is the size of the beamwidth in millimeters. The r^2 value for the linear regression line is 0.96. For the threshold water-breaking rarefactional pressure for the continuous wave, there is a statistically significant difference (p -value < 0.05) in the threshold water-breaking rarefactional pressure as the beamwidth increases.

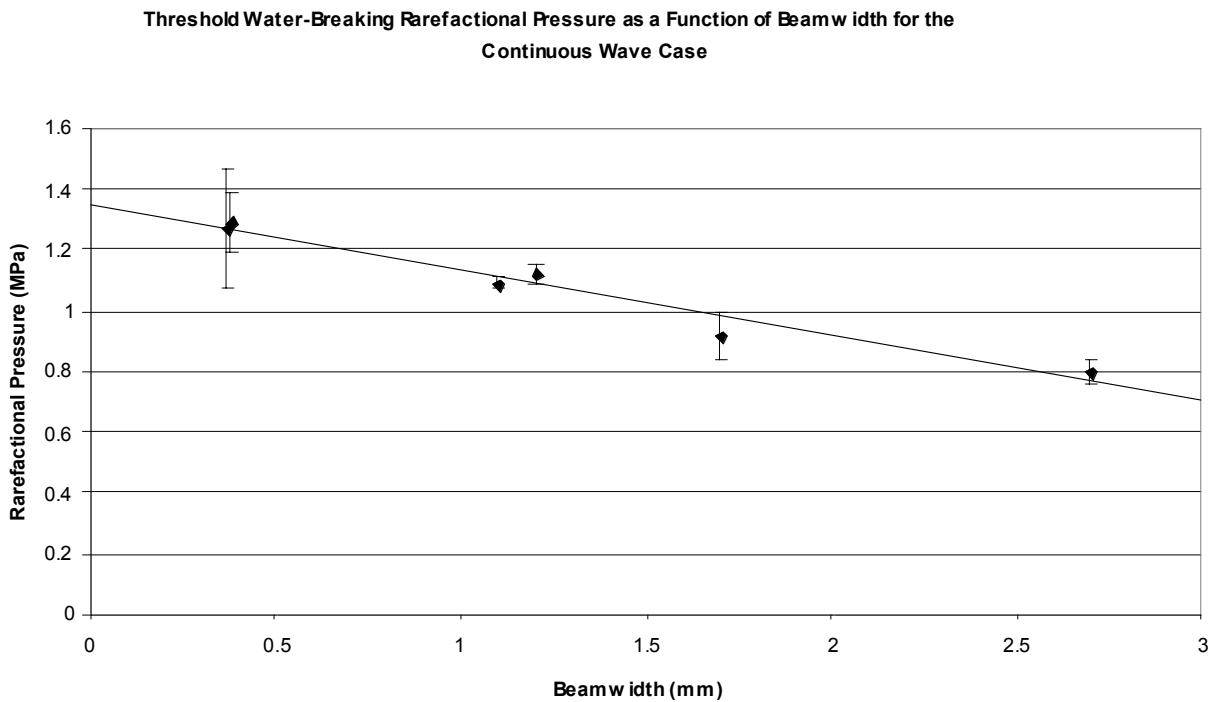


Figure 4.4 Threshold Water-Breaking Rarefactional Pressure for the Continuous Wave Case with Beamwidth Dependency and a Linear Regression Line

Figure 4.5 (pulsed wave case, PRF = 1 kHz) shows an overall decrease in the threshold water-breaking rarefactional pressure with increasing beamwidth. This is consistent with the trend for the continuous wave case.

Threshold Water-Breaking Rarefactional Pressure as a Function of Beamwidth for
PRF = 1 kHz

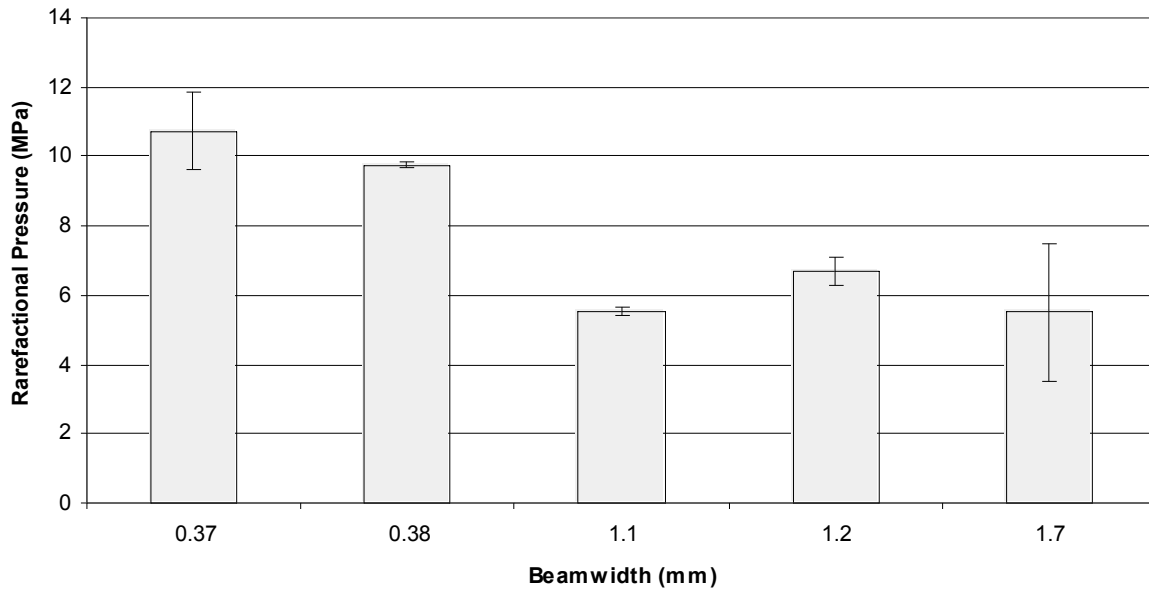


Figure 4.5 Threshold Water-Breaking Rarefactional Pressure for the Pulsed Case (PRF = 1 kHz) with Beamwidth Dependency

Figure 4.6 (pulsed wave case, PRF = 500 Hz) shows an overall decrease in the threshold water-breaking rarefactional pressure with increasing beamwidth. This is consistent with the trend for the continuous wave (Figure 4.3) and pulsed wave case at 1 kHz (Figure 4.5).

Threshold Water-Breaking Rarefactional Pressure as a Function of Beam width for
PRF = 500 Hz

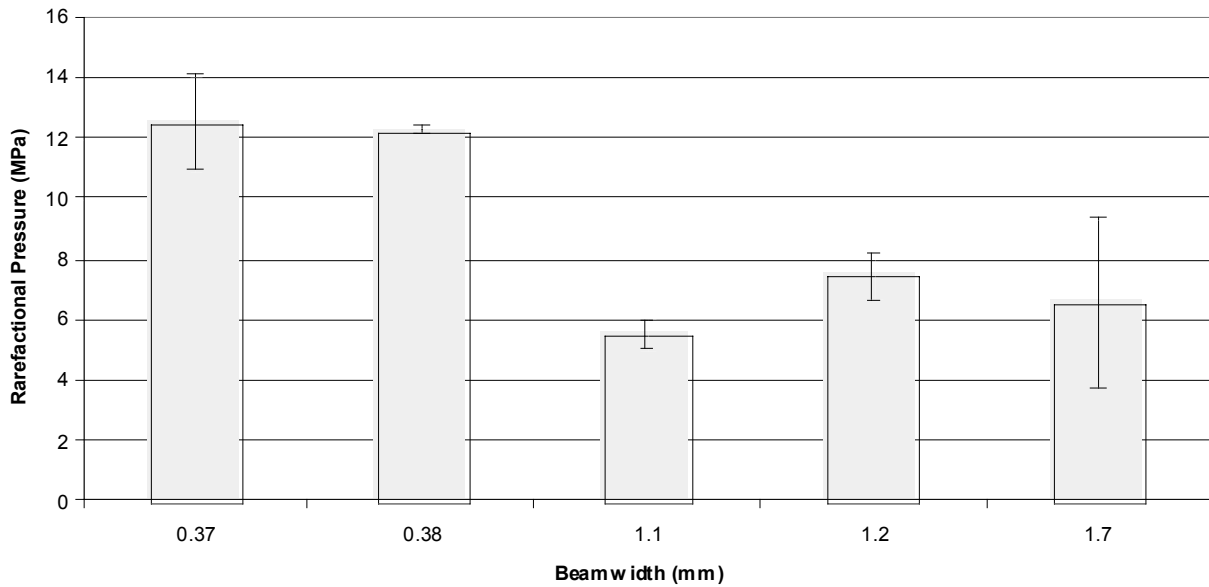


Figure 4.6 Threshold Water-Breaking Rarefactional Pressure for the Pulsed Case (PRF = 500 Hz) with Beamwidth Dependency

Figure 4.7 shows the threshold water-breaking rarefactional pressure for the two pulsed wave case plotted as a function of increasing beamwidth. The top regression line (PRF = 500 Hz) in Figure 4.7 has the equation $P = -5.0821b + 13.670$. The r^2 value for the linear regression line for PRF = 500 Hz is 0.78. The lower regression line (PRF = 1 kHz) in the same figure has the equation $P = -3.939 + 11.391$. The r^2 value for the linear regression line for PRF = 1 kHz is 0.85. There is a statistically significant difference (p -value < 0.05) in the threshold water-breaking rarefactional pressure for both pulsed cases as a function of beamwidth.

Threshold Water-Breaking Rarefactional Pressure as a Function of Beamwidth for the Pulsed Cases

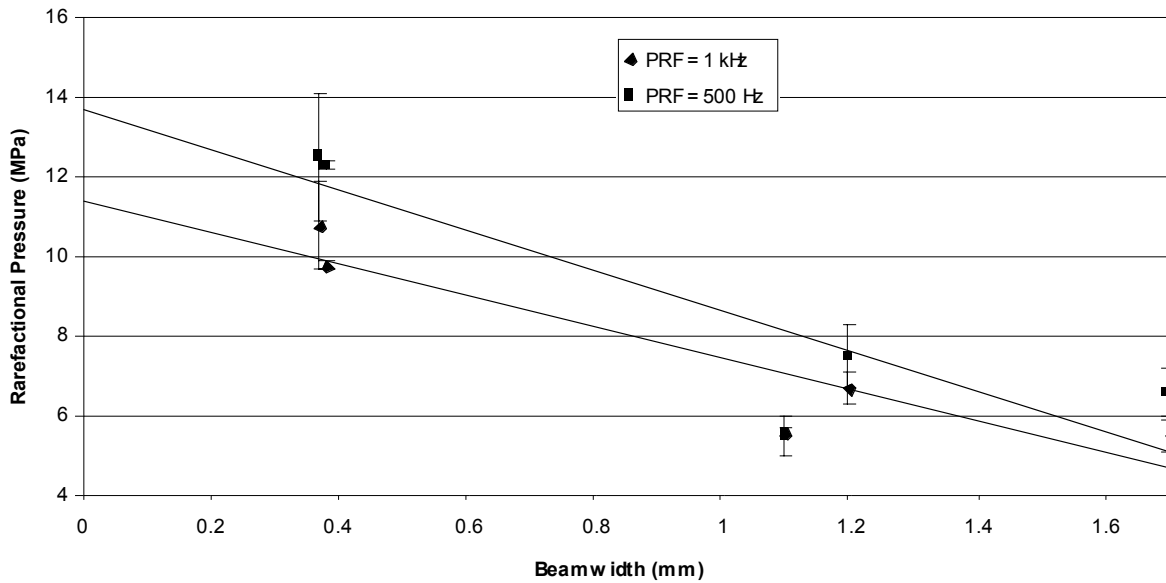


Figure 4.7 Threshold Water-Breaking Rarefactional Pressure for the Pulsed Wave Case with Beamwidth Dependency and a Linear Regression Line

In addition to measuring the threshold water-breaking rarefactional pressure, the threshold water-breaking compressional pressure for all three cases (continuous wave, PRF = 1 kHz, and PRF = 500 Hz) was studied. Figures 4.8-4.12 show how the threshold water-breaking compressional pressure changes with a change in the beamwidth. Figure 4.8 is the threshold water-breaking compressional pressure for the continuous wave case and Figure 4.10 is the threshold water-breaking compressional pressure for the pulsed case, where the pulse repetition frequency is 1 kHz. Figure 4.11 is the threshold water-breaking compressional pressure for the pulsed case, where the pulse repetition frequency is 500 Hz.

Figure 4.8 (continuous wave case) shows an overall decrease in the threshold water-breaking compressional pressure as beamwidth increases. The outlier is the 2.7 mm beamwidth, which increases.

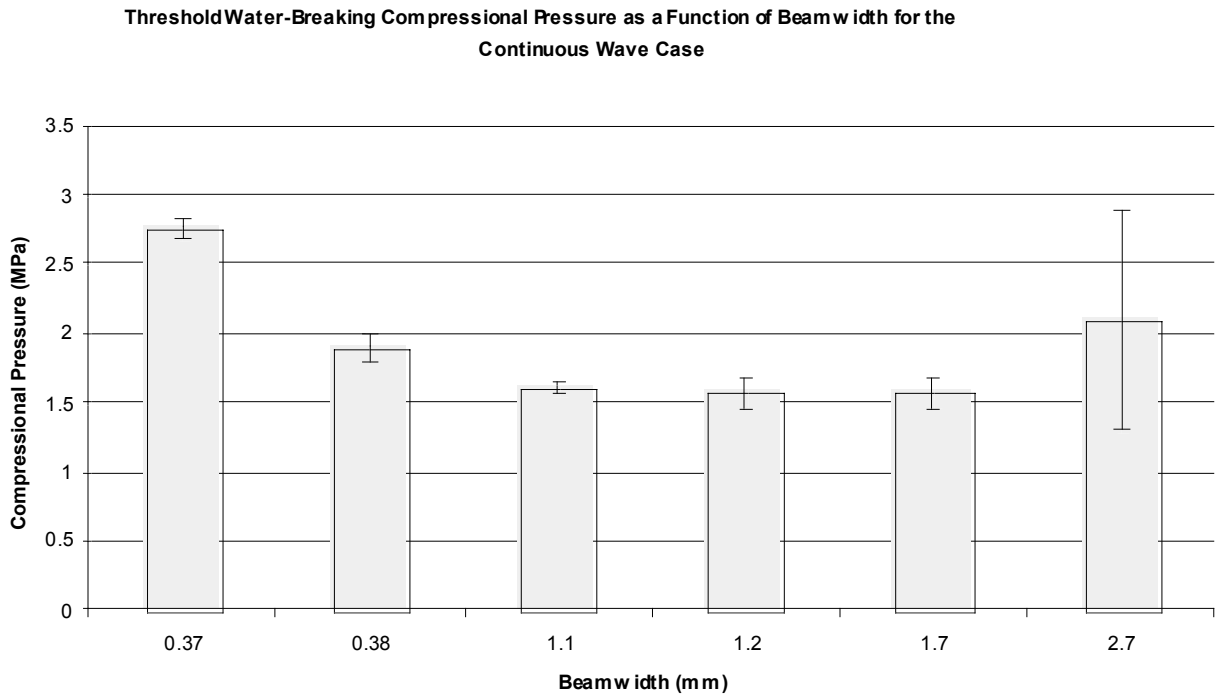


Figure 4.8 Threshold Water-Breaking Compressional Pressure for the Continuous Wave Case with Beamwidth Dependency

Figure 4.9 shows the threshold water-breaking compressional pressure for the continuous wave case plotted as a function of increasing beamwidth. The regression line in Figure 4.9 has the equation $P = -0.196b + 2.137$. The r^2 value for the linear regression line is 0.14. There is a statistically significant difference ($p\text{-value} > 0.05$) in the threshold water-breaking rarefactional pressure for the continuous wave case as a function of beamwidth.

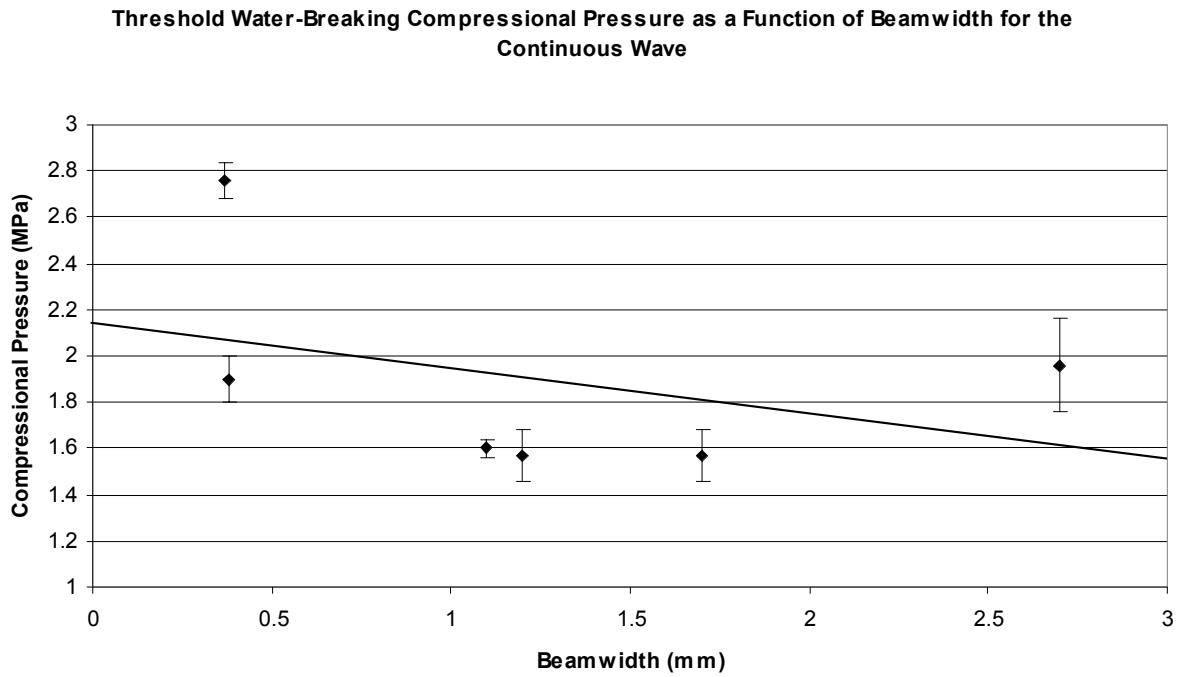


Figure 4.9 Threshold Water-Breaking Compressional Pressure for the Continuous Wave Case with Beamwidth Dependency and a Linear Regression Line

Figure 4.10 (pulsed wave case, PRF = 1 kHz) shows an overall decrease in the threshold water breaking compressional pressure with increasing beamwidth. This is consistent with the trend for the continuous wave (Figure 4.8)

Threshold Water-Breaking Compressional Pressure as a Function of Beam width for
PRF = 1 kHz

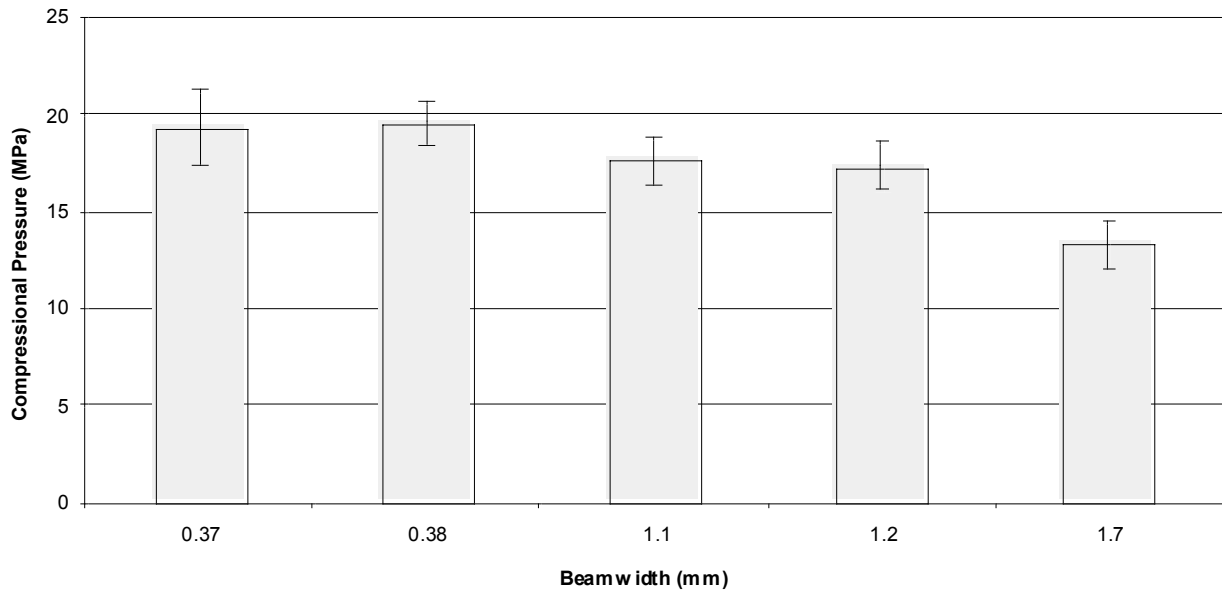


Figure 4.10 Threshold Water-Breaking Compressional Pressure for the Pulsed Case (PRF = 1 kHz) with Beamwidth Dependency

Figure 4.11 (pulsed wave case, PRF = 500 Hz) shows an overall decrease in the water-breaking compressional pressure with increasing beamwidth. This is consistent with the trend for the continuous wave (Figure 4.8) and the pulsed wave case at 1 kHz (Figure 4.10).

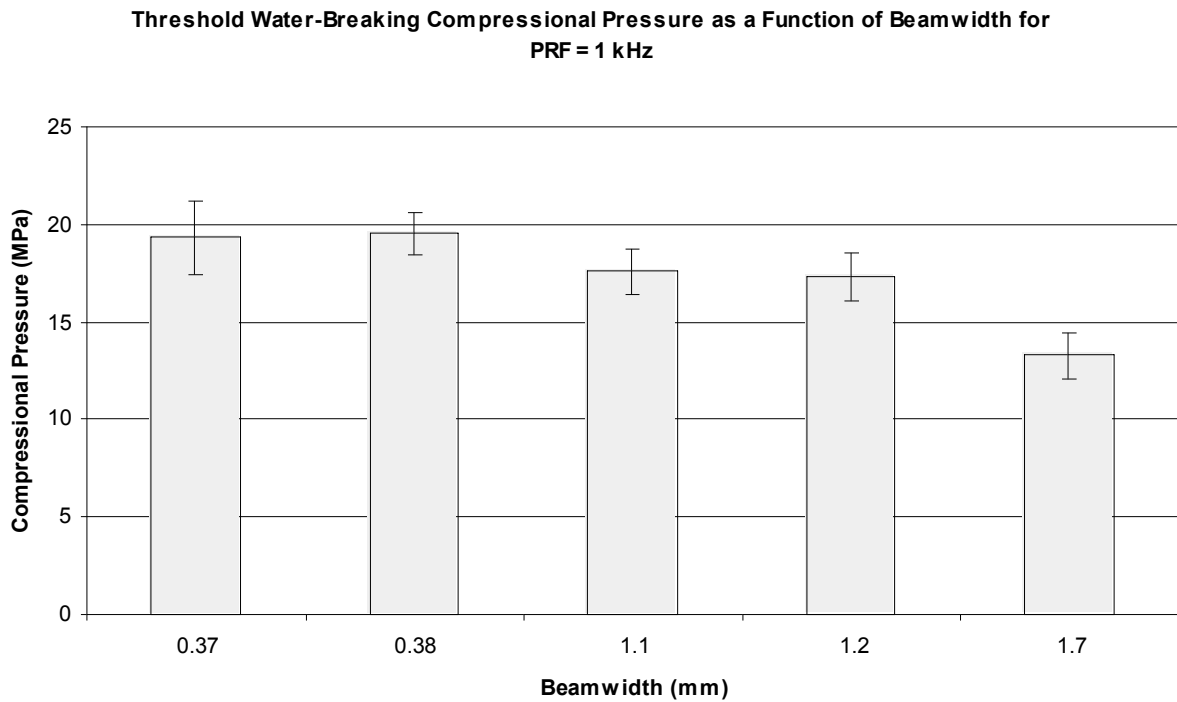


Figure 4.11 Threshold Water-Breaking Compressional Pressure for the Pulsed Case (PRF = 500 Hz) with Beamwidth Dependency

Figure 4.12 shows the threshold water-breaking compressional pressure for the two pulsed wave case plotted as a function of increasing beamwidth. The top regression line (PRF = 500 Hz) in Figure 4.12 has the equation $P = -4.153b + 21.357$. The r^2 value for the linear regression line for PRF = 500 Hz is 0.89. The lower regression line (PRF = 1 kHz) in the same figure has the equation $P = -3.218b + 22.955$. The r^2 value for the linear regression line for PRF = 1 kHz is 0.90. There is a statistically significant difference (p-value < 0.05) in the threshold water-breaking compressional pressure for both pulsed cases as a function of beamwidth.

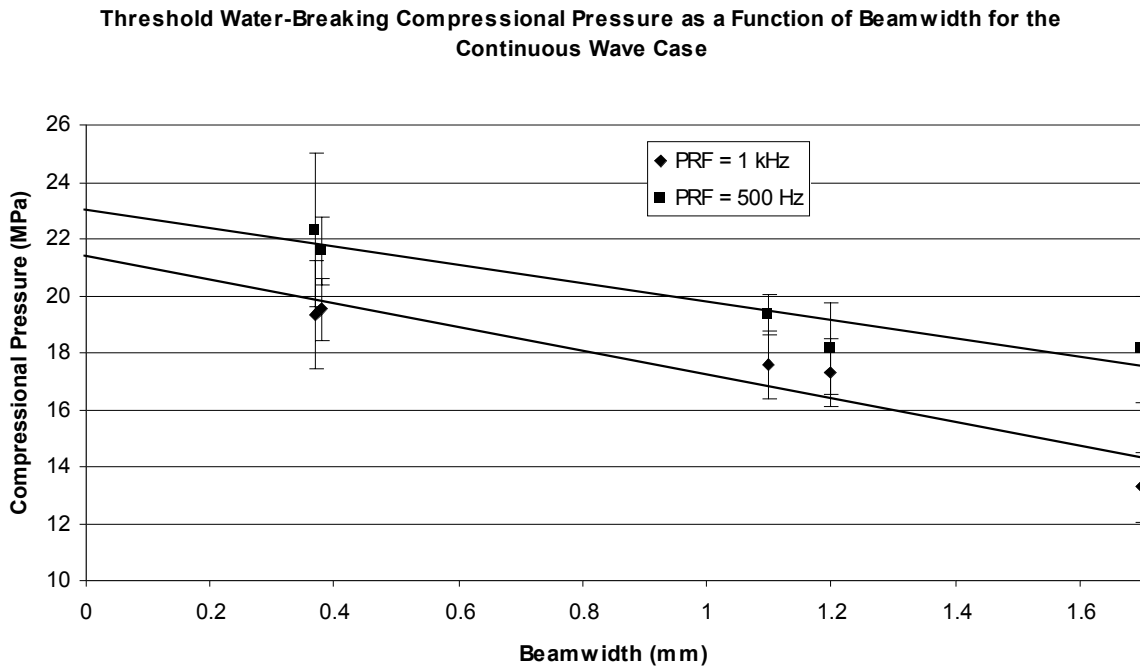


Figure 4.12 Threshold Water-Breaking Compressional Pressure for the Pulsed Wave Case with Beamwidth Dependency and a Linear Regression Line

In addition to observing how pulse repetition frequency and beamwidth affect the threshold water-breaking rarefactional and compressional pressures, the effect of the ultrasonic frequency on threshold water-breaking rarefactional and compressional pressures were also studied.

The effect ultrasonic frequency has on the threshold water-breaking rarefactional pressure can be seen in Figure 4.13-4.17. These figures show how the threshold water-breaking rarefactional pressure (y-axis) changes with a change in the frequency (x-axis). Figure 4.13 is the threshold water-breaking rarefactional pressure for the continuous wave case and Figure 4.15 is the threshold water-breaking rarefactional pressure for the pulsed case, where the pulse repetition frequency is 1 kHz. Figure 4.16 is the threshold water-breaking rarefactional pressure for the pulsed case, where the pulse repetition frequency is 500 Hz.

Figure 4.13 (continuous wave case) shows that no trend in the pressure can be observed as the frequency increases.

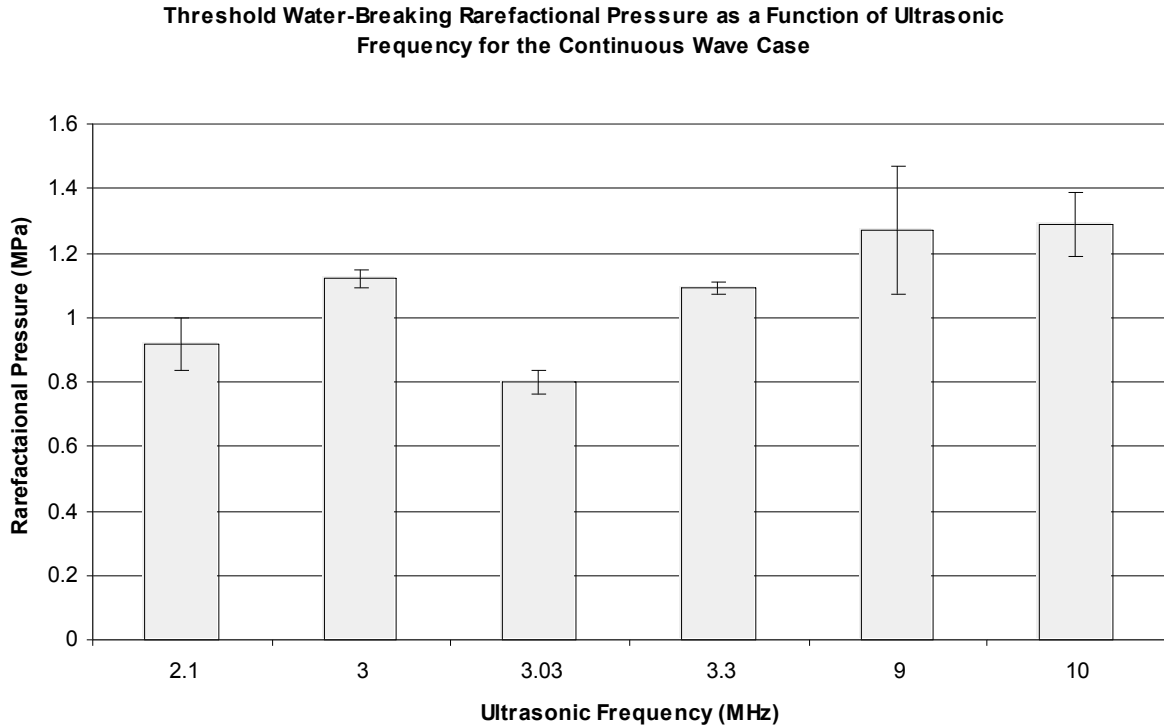


Figure 4.13 Threshold Water-Breaking Rarefactional Pressure for the Continuous Wave Case with Ultrasonic Frequency Dependency

Figure 4.14 shows the threshold water-breaking rarefactional pressure for the continuous wave case plotted as a function of increasing ultrasonic frequency. The regression line in Figure 4.14 has the equation $P = 0.0454f + 0.852$, where f is the ultrasonic frequency. The r^2 value for the linear regression line is 0.67. There is a statistically significant difference (p -value < 0.05) in the threshold water-breaking rarefactional pressure as a function of the ultrasonic frequency.

Threshold Water-Breaking Rarefactional Pressure as a Function of Ultrasonic Frequency for the Continuous Wave Case

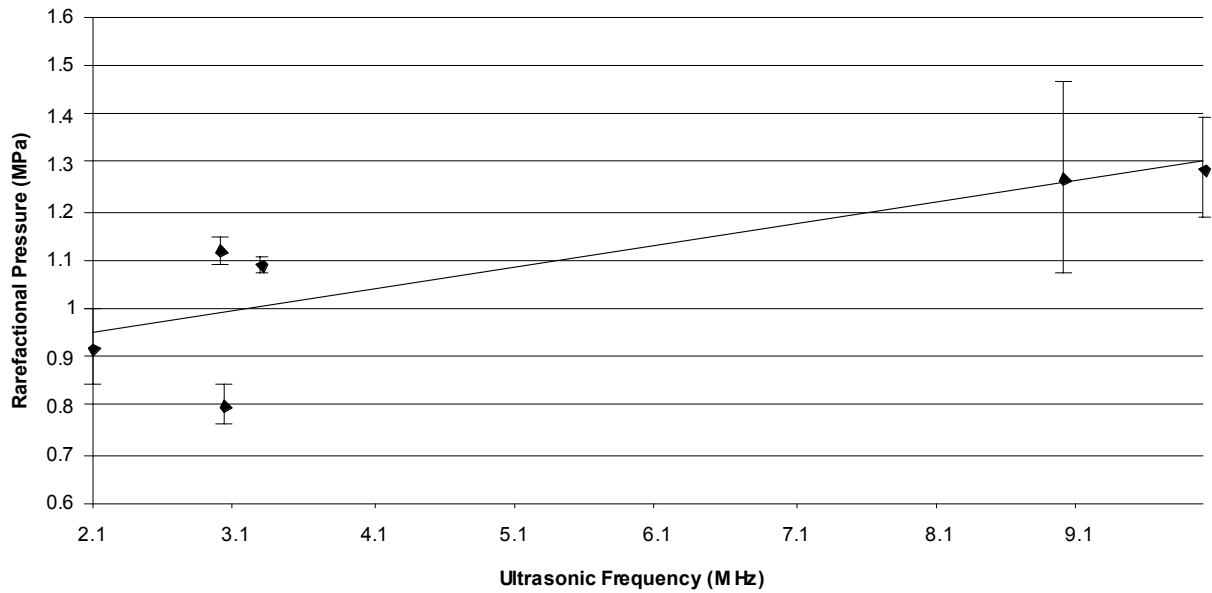


Figure 4.14 Threshold Water-Breaking Rarefactional Pressure for the Continuous Wave Case with Ultrasonic Frequency Dependency and a Linear Regression Line

Figure 4.15 (pulsed wave case, PRF = 1 kHz) shows that for lower frequencies (2.1, 3, and 3.3 MHz), there is no trend in the threshold water-breaking rarefactional pressure. However, the threshold water-breaking rarefactional pressure at high frequencies is much greater than at lower frequencies.

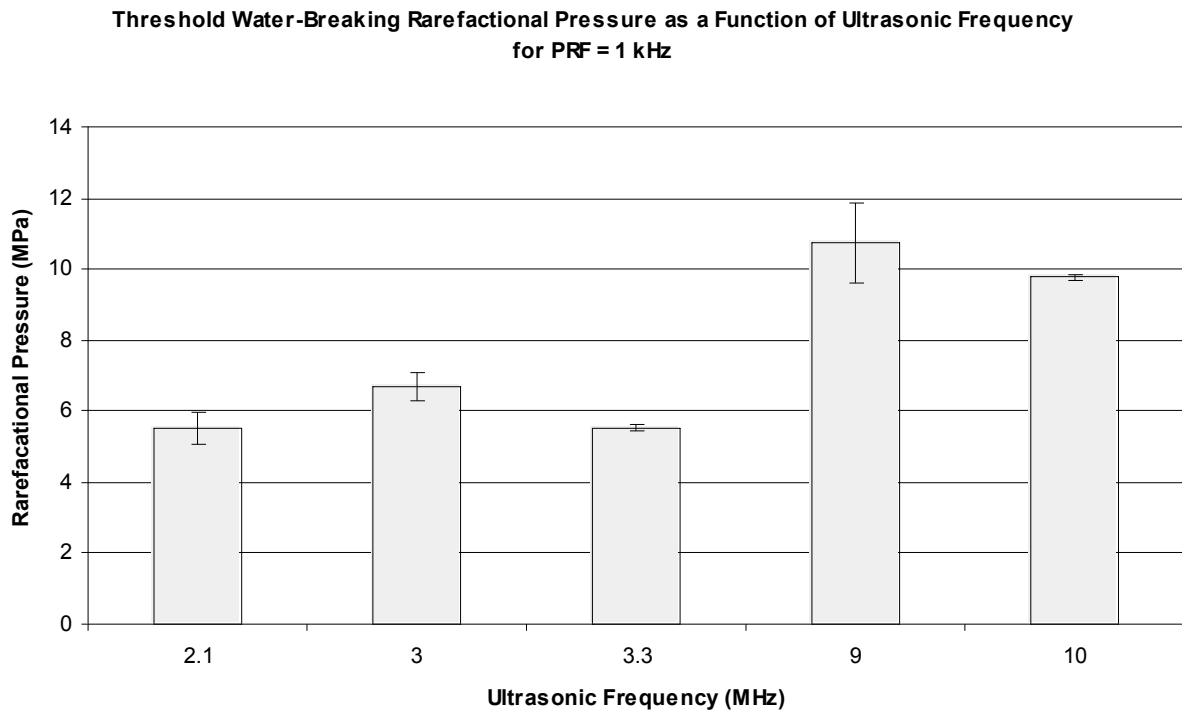


Figure 4.15 Threshold Water-Breaking Rarefactional Pressure for the Pulsed Case (PRF = 1 kHz) with Ultrasonic Frequency Dependency

Figure 4.16 (pulsed wave case, PRF = 500 Hz) shows that for lower frequencies (2.1- 3.3 MHz), there is no trend in the threshold water-breaking rarefactional pressure. However, the threshold water-breaking rarefactional pressure at high frequencies is much greater than at lower frequencies. This trend is consistent with that for the pulsed wave case at 1 kHz.

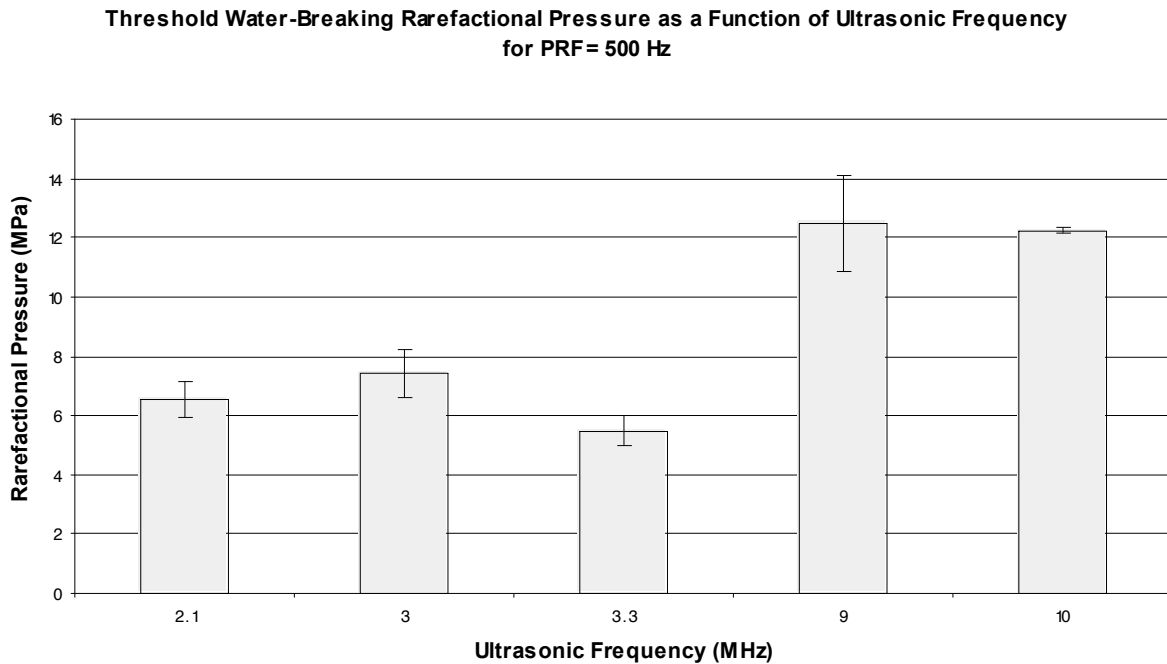


Figure 4.16 Threshold Water-Breaking Rarefactional Pressure for the Pulsed Case (PRF = 500 Hz) with Ultrasonic Frequency Dependency

Figure 4.17 shows the threshold water-breaking rarefactional pressure for the two pulsed wave case plotted as a function of increasing ultrasonic frequency. The top regression line (PRF = 500 Hz) in Figure 4.17 has the equation $P = 0.850f + 4.184$. The r^2 value for the linear regression line for PRF = 500 Hz is 0.92. The lower regression line (PRF = 1 kHz) in the same figure has the equation $P = 0.628f + 4.207$. The r^2 value for the linear regression line for PRF = 1 kHz is 0.91. There is a statistically significant difference (p -value < 0.05) in the threshold water-breaking compressional pressure for both pulsed cases as a function of ultrasonic frequency.

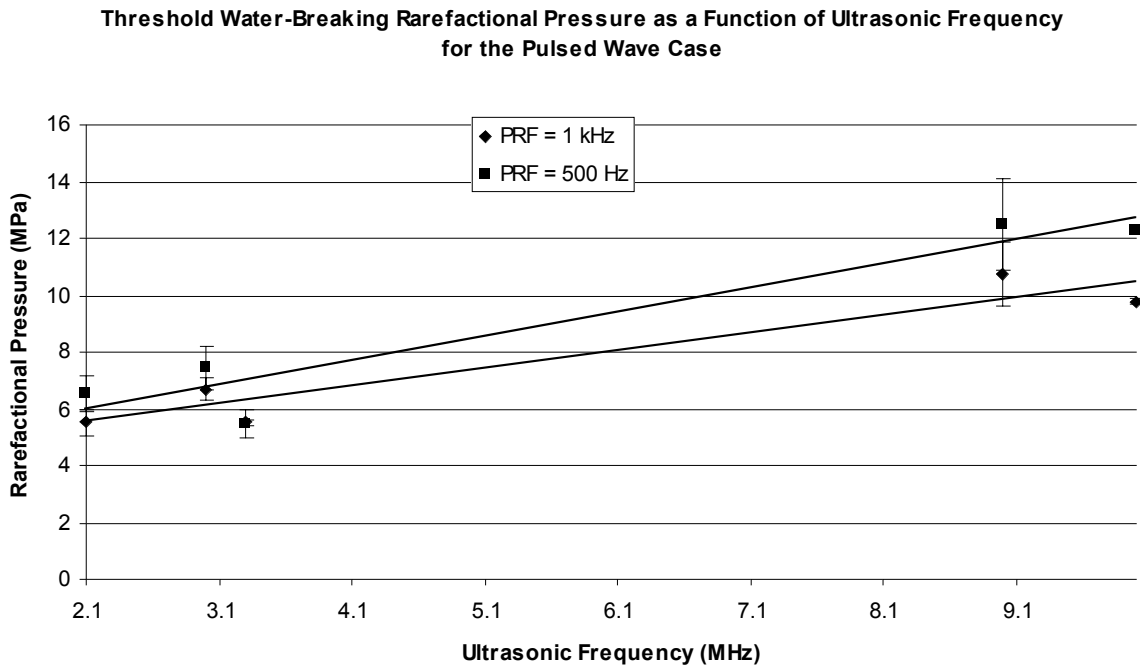


Figure 4.17 Threshold Water-Breaking Rarefactional Pressure for the Pulsed Wave Case with Ultrasonic Frequency Dependency and a Linear Regression Line

In addition to measuring the threshold water-breaking rarefactional pressure, the threshold water-breaking compressional pressure for all three cases (continuous wave, PRF = 1 kHz, and PRF = 500 Hz) was studied. Figures 4.18-4.22 show how the threshold water-breaking compressional pressure changes with a change in the ultrasonic frequency. Figure 4.18 is the threshold water-breaking compressional pressure for the continuous wave case and Figure 4.20 is the threshold water-breaking compressional pressure for the pulsed case, where the pulse repetition frequency is 1 kHz. Figure 4.21 is the threshold water-breaking compressional pressure for the pulsed case, where the pulse repetition frequency is 500 Hz.

Figure 4.18 (continuous wave case) does not show an overall decrease in the threshold water-breaking compressional pressure as the frequency increases.

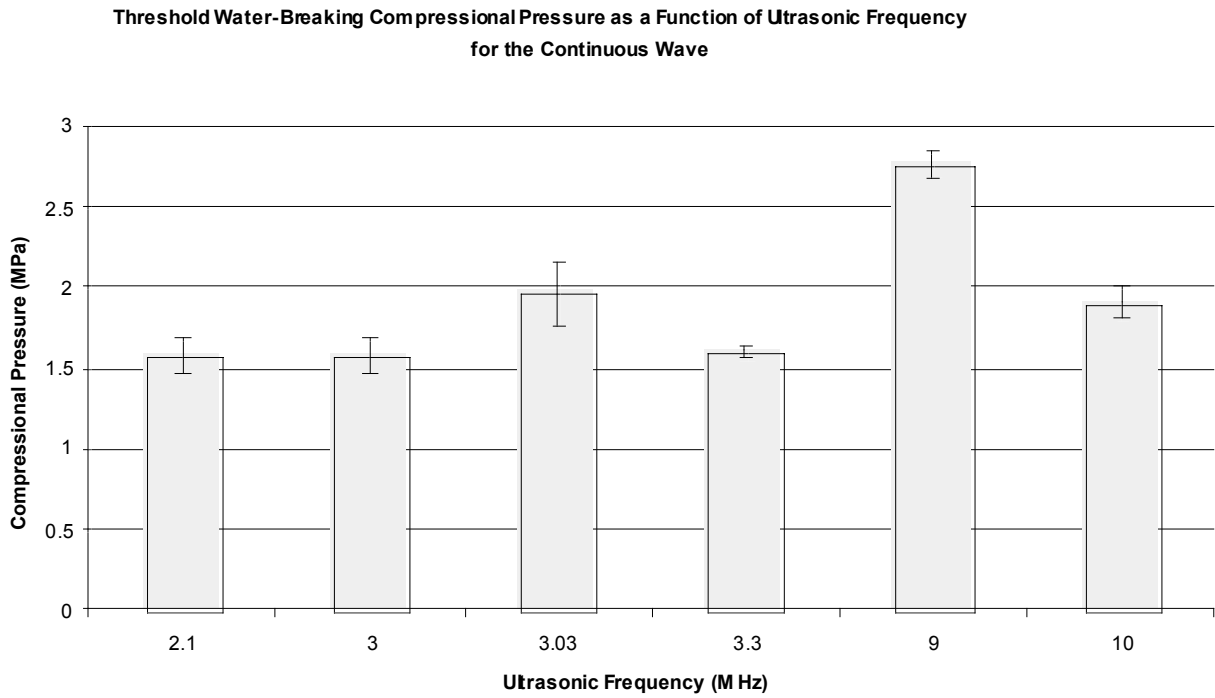


Figure 4.18 Threshold Water-Breaking Compressional Pressure for the Continuous Wave Case with Ultrasonic Frequency Dependency

Figure 4.19 shows the threshold water-breaking compressional pressure for the continuous wave case plotted as a function of increasing ultrasonic frequency. The regression line in Figure 4.19 has the equation $P = 0.09063f + 1.434$. The r^2 value for the linear regression line is 0.47. There is not a statistically significant difference ($p\text{-value} > 0.05$) in the threshold water-breaking compressional pressure as a function of the ultrasonic frequency.

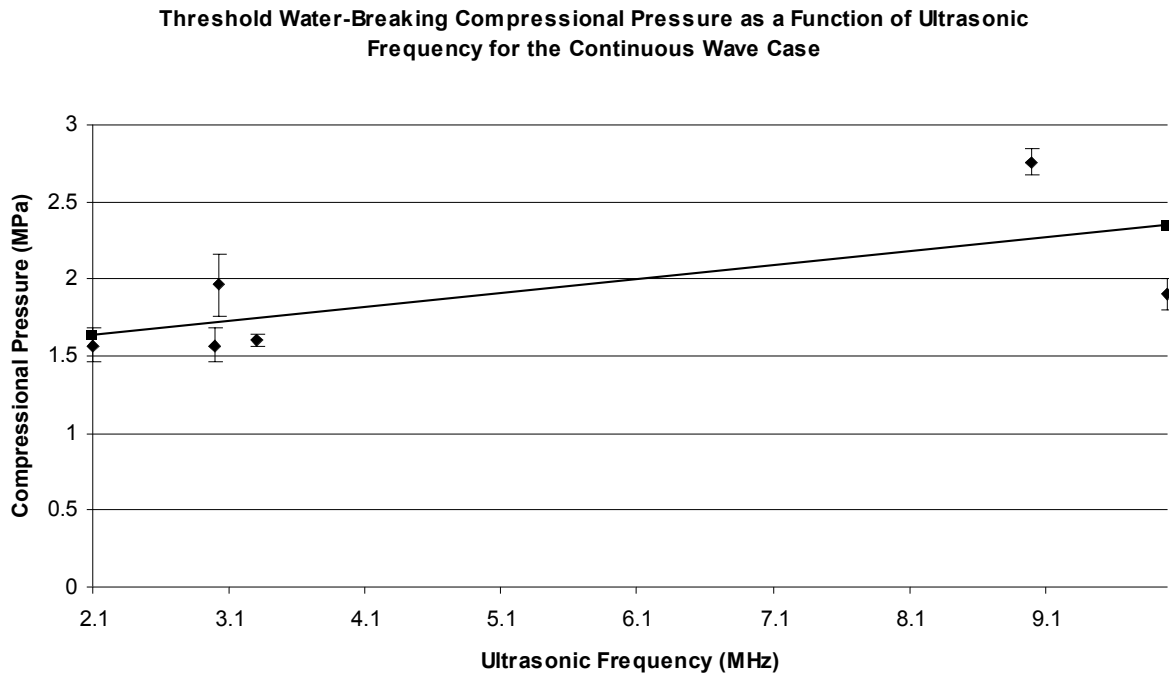


Figure 4.19 Threshold Water-Breaking Compressional Pressure for the Continuous Wave Case with Ultrasonic Frequency Dependency and a Linear Regression Line

Figure 4.20 (pulsed wave case, PRF = 1 kHz) shows an overall increase in the threshold water-breaking compressional pressure as the frequency increases.

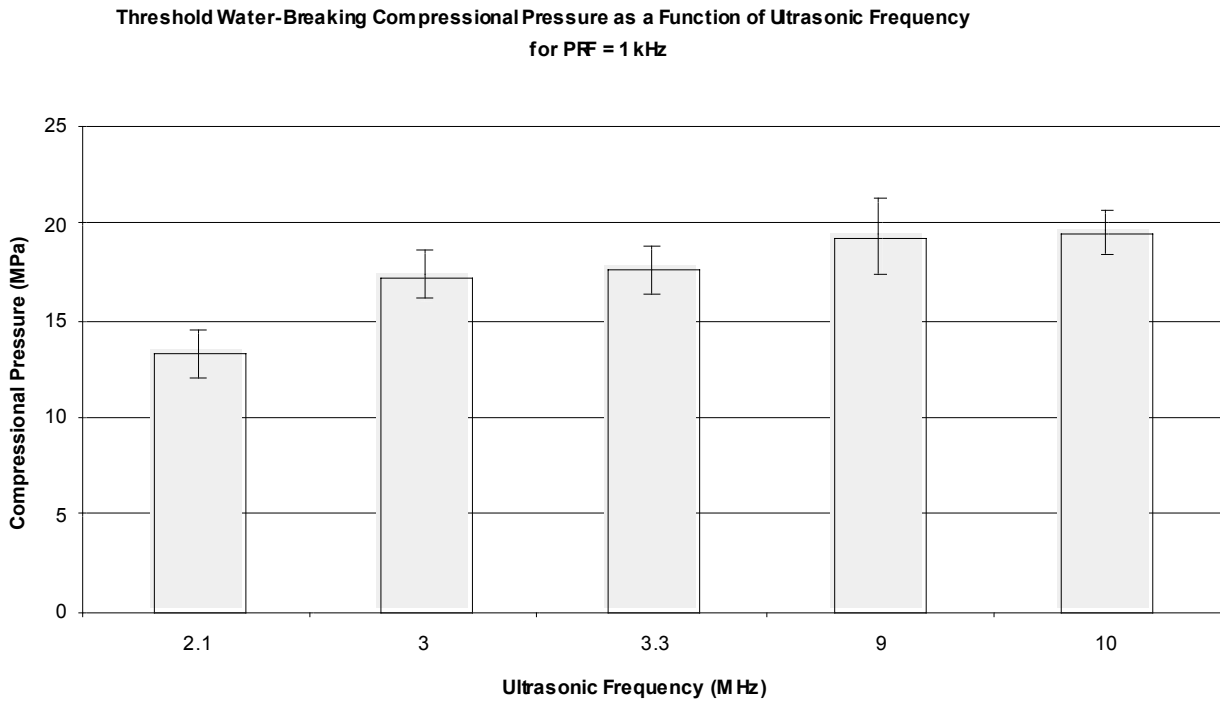


Figure 4.20 Threshold Water-Breaking Rarefactional Pressure for the Pulsed Case (PRF = 1 kHz) with Ultrasonic Frequency Dependency

Figure 4.21 (pulsed wave case, PRF = 500 Hz) shows an overall increase in the threshold water-breaking compressional pressure as the frequency increases. This trend is consistent with that for the pulsed wave case at 1 kHz (Figure 4.20).

**Threshold Water-Breaking Compressional Pressure as a Function of Ultrasonic Frequency
for PRF = 500 Hz**

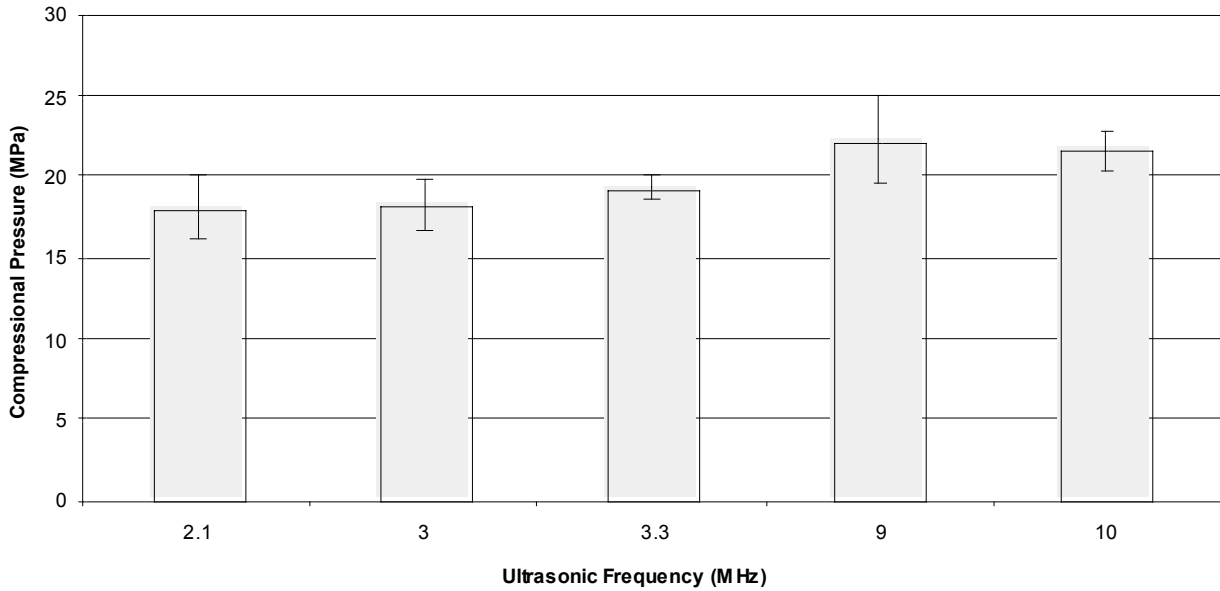


Figure 4.21 Threshold Water-Breaking Rarefactional Pressure for the Pulsed Case (PRF = 500 Hz) with Ultrasonic Frequency Dependency

Figure 4.22 shows the threshold water-breaking compressional pressure for the two pulsed wave case plotted as a function of increasing ultrasonic frequency. The top regression line (PRF = 500 Hz) in Figure 4.20 has the equation $P = 0.502f + 17.146$. The r^2 value for the linear regression line for PRF = 500 Hz is 0.92. The lower regression line (PRF = 1 kHz) in the same figure has the equation $P = 0.548f + 14.408$. The r^2 value for the linear regression line for PRF = 1 kHz is 0.65. There is a statistically significant difference (p-value < 0.05) in the threshold water-breaking compressional pressure for the pulsed case, where the PRF = 500 Hz, as a function of ultrasonic frequency. For the pulsed case, where the PRF = 1 kHz, there is not a statistically significant difference (p-value > 0.05) in the threshold water-breaking compressional pressure as a function of ultrasonic frequency.

Threshold Water-Breaking Compressional Pressure as a Function of Ultrasonic Frequency for the Pulsed Wave Case

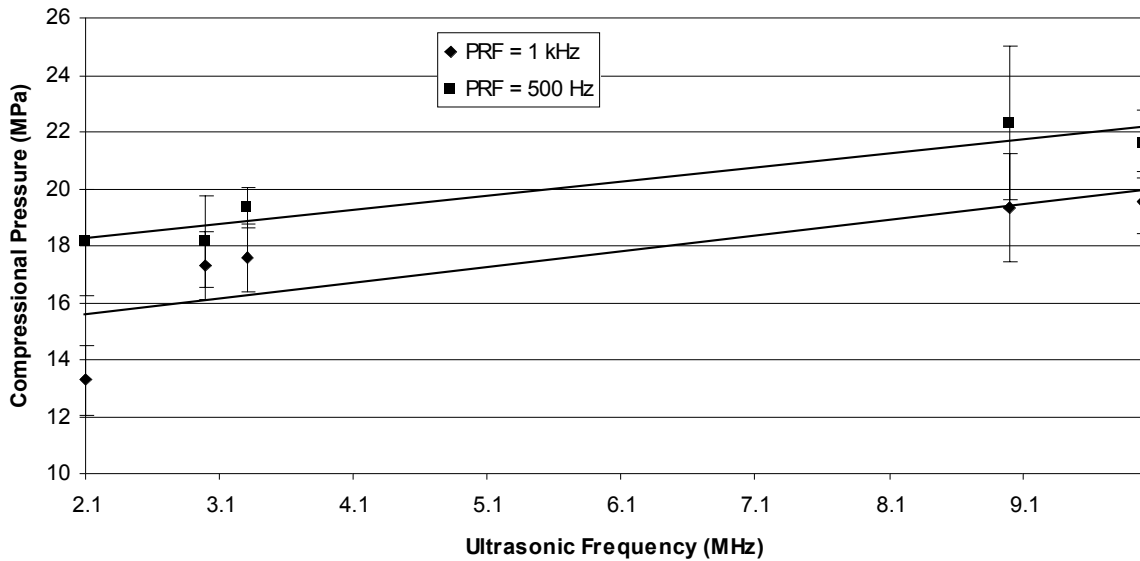


Figure 4.22 Threshold Water-Breaking Compressional Pressure for the Pulsed Wave Case with Ultrasonic Frequency Dependency and a Linear Regression Line

The radiation force, as explained in Chapter 1 and 2, was determined from the voltage intensity integral. The threshold water-breaking voltage intensity integral was determined by performing a linear regression analysis over the data points where the transducer was calibrated. Table 4.5 shows the voltage intensity integral equations for the corresponding threshold water-breaking voltage values from Table 4.3 at each setting.

Settings	VII Equation
Blue 3.0 MHz, CW	$VII = 6.48E-10 \cdot v - 2.32E-9$
Blue 3.0 MHz, PRF= 1 kHz	$VII = 2.25E-8 \cdot v - 6.01E-6$
Blue 3.0 MHz, PRF= 500 Hz	$VII = 6.23E-9 \cdot v - 1.08E-6$
Blue 9.0 MHz, CW	$VII = 8.65E-10 \cdot v - 1.20E-7$
Blue 9.0 MHz, PRF= 1 kHz	$VII = 1.23E-9 \cdot v - 1.48E-8$
Blue 9.0 MHz, PRF= 500 Hz	$VII = 2.49E-9 \cdot v - 2.44E-7$
Orange 3.3 MHz, CW	$VII = 1.80E-9 \cdot v - 1.93E-8$
Orange 3.3 MHz, PRF= 1 kHz	$VII = 4.43E-9 \cdot v - 4.15E-8$
Orange 3.3 MHz, PRF= 500 Hz	$VII = 9.21E-8 \cdot v - 2.11E-6$
Orange 10 MHz, CW	$VII = 3.18E-9 \cdot v - 3.86E-7$
Orange 10 MHz, PRF= 1 kHz	$VII = 7.84E-9 \cdot v - 2.55E-6$

Orange 10 MHz, PRF= 500 Hz	$VII = 1.05E-8*v - 4.16E-6$
Red 2.1 MHz, CW	$VII = 2.37E-9*v - 3.71E-8$
Red 2.1 MHz, PRF= 1 kHz	$VII = 9.79E-9*v - 3.75E-7$
Red 2.1 MHz, PRF= 500 Hz	$VII = 1.77E-8*v - 1.24E-6$
Yellow 3.03 MHz, CW	$VII = 6.80E-10*v - 1.76E-8$
Yellow 3.03 MHz, PRF= 11 kHz	$VII = 6.02E-10*v - 4.46E-8$
Yellow 3.03 MHz, PRF= 9 kHz	$VII = 5.12E-10*v - 7.16E-8$

Table 4.5 Equations for the Threshold Water-Breaking Voltage Intensity Integral, v is the Threshold Water-Breaking Voltage Value

A figure of the threshold water-breaking radiation force for the continuous and pulsed wave cases is shown in Figure 4.23.

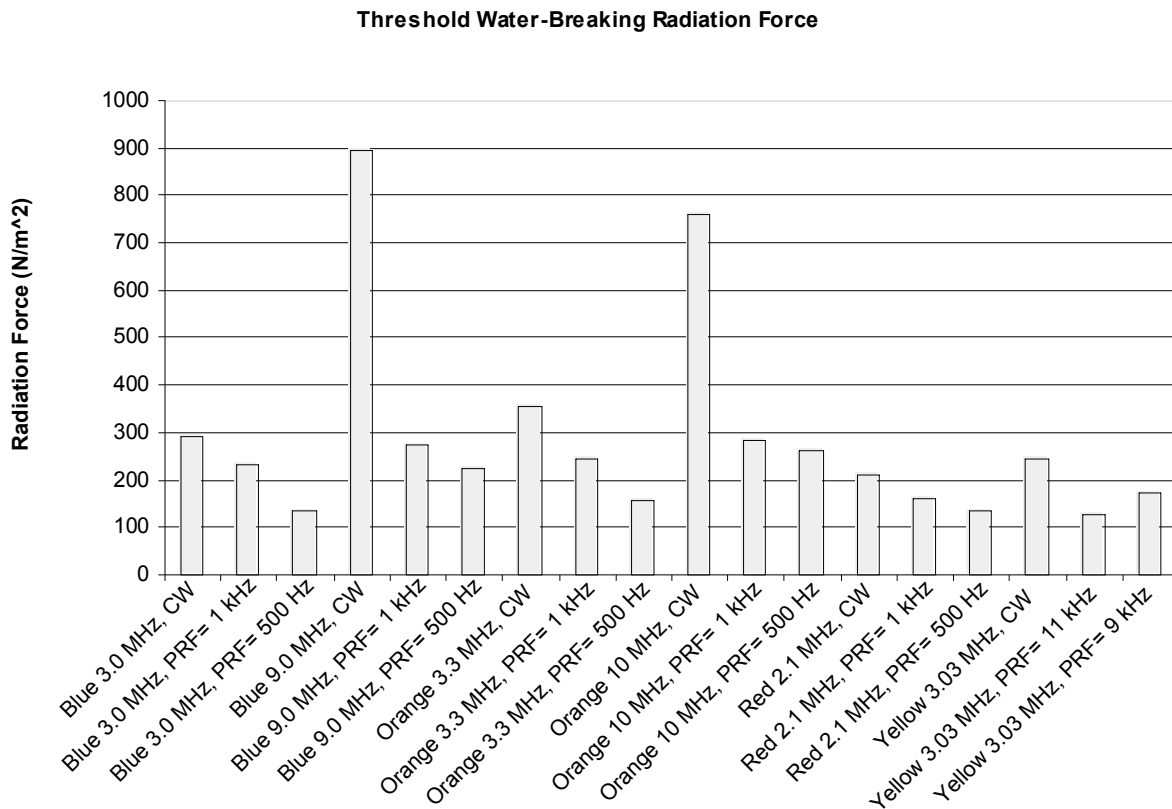


Figure 4.23 Threshold Water-Breaking Radiation Force

The overall trend for the threshold water-breaking radiation force is that the continuous wave threshold water-breaking radiation force is greater than the threshold water-breaking radiation force for the two pulsed wave conditions. The overall trend is that the threshold water-

breaking radiation force for the lower pulse repetition frequency for each transducer is the smaller than the threshold water-breaking radiation force for the higher pulse repetition frequency.

The threshold water-breaking radiation force data for the continuous and pulsed wave cases were analyzed by using duty factor. Figure 4.24 shows how the threshold water-breaking radiation force varies as a function of duty factor. A linear regression analysis was also performed and the equations for the six lines are:

- Blue, 3.0 MHz: $F = 110.63 \cdot DF + 181.76$ $r^2 = 0.64$
- Blue, 9.0 MHz: $F = 654.50 \cdot DF + 240.34$ $r^2 = 0.99$
- Orange, 3.3 MHz: $F = 154.15 \cdot DF + 198.72$ $r^2 = 0.79$
- Orange, 10 MHz: $F = 491.16 \cdot DF + 266.92$ $r^2 = 0.99$
- Red, 2.1 MHz: $F = 62.29 \cdot DF + 147.80$ $r^2 = 0.89$
- Yellow, 3.03 MHz: $F = 112.37 \cdot DF + 133.94$ $r^2 = 0.85$

F is the equation for radiation force as a function of duty factor, DF.

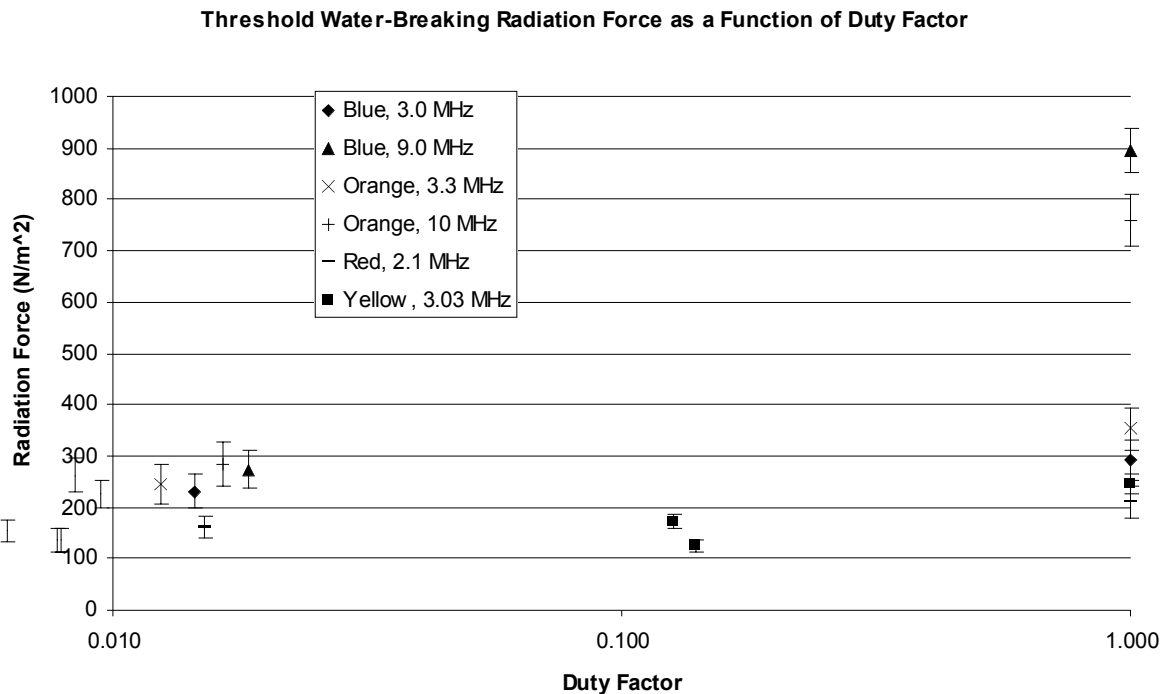


Figure 4.24 Threshold Water-Breaking Radiation Force as a Function of Duty Factor

The beamwidth of an ultrasonic beam has been reported to affect the threshold of lung damage in adult rats [O'Brien et al., 2001]. Thus, there is some importance in determining if and how beamwidth affects the threshold water-breaking radiation force.

Figure 4.25 shows the threshold water-breaking radiation force as a function of beamwidth for the continuous wave case. The overall trend is as beamwidth increases, the threshold water-breaking radiation force decrease. The beamwidth varies from 0.37 – 2.7 mm, with the smallest beamwidth represented on the far left of Figure 4.25 and the largest beamwidth represented on the far right of the same figure. The threshold water-breaking radiation force for the smallest beamwidth is 894 N/m². The threshold water-breaking radiation force for the largest beamwidth is 210 N/m².

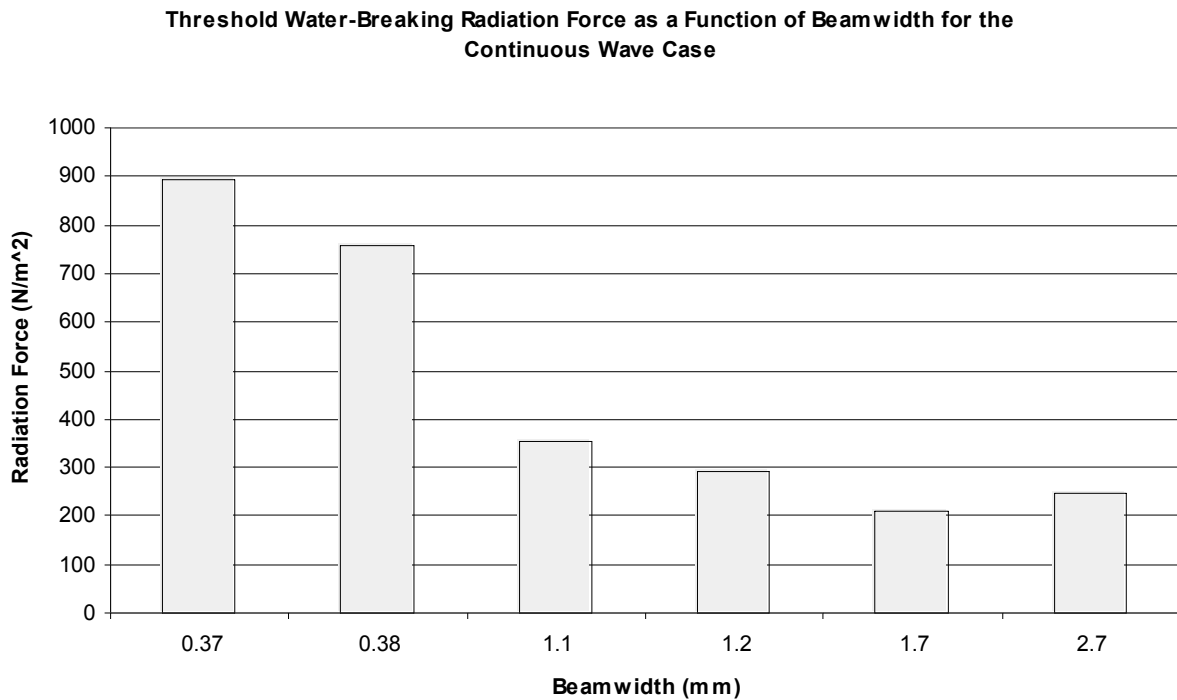


Figure 4.25 Threshold Water-Breaking Radiation Force due to Beamwidth for the Continuous Wave Case

Figure 4.26 shows the threshold water-breaking radiation force for the continuous wave case plotted as a function of increasing beamwidth. The regression line in Figure 4.26 has the

equation $F = -277.872b + 862.509$. The r^2 value for the linear regression line is 0.68. There is a statistically significant difference (p -value < 0.05) in the threshold water-breaking compressional pressure as a function of the beamwidth.

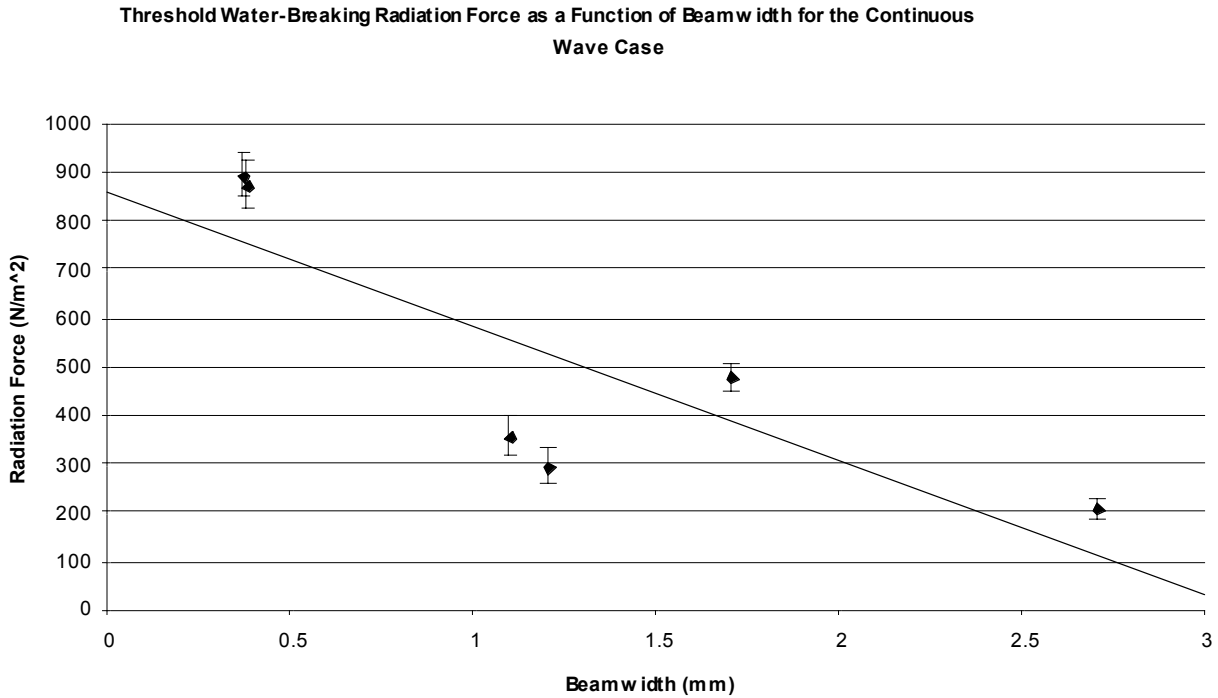


Figure 4.26 Threshold Water-Breaking Radiation Force for the Continuous Wave Case with Beamwidth Dependency and a Linear Regression Line

Figure 4.27 (pulsed wave case, PRF = 1 kHz) also shows the threshold water-breaking radiation force as a function of beamwidth. The overall trend is that as the beamwidth increases, the threshold water-breaking radiation force decreases. This is consistent with the results for the continuous wave case (Figure 4.25).

Threshold Water-Breaking Radiation Force as a Function of Beamwidth for the PRF = 1 kHz

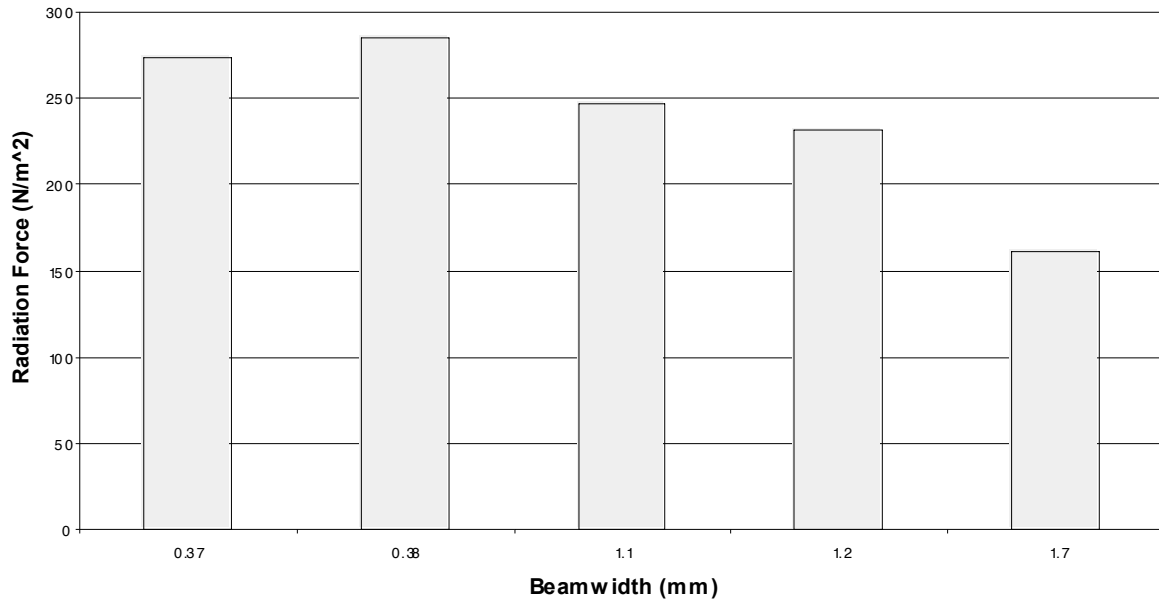


Figure 4.27 Threshold Water-Breaking Radiation Force due to Beamwidth for the PRF = 1 kHz Case

Figure 4.28 (pulsed wave case, PRF = 500 Hz) shows an overall decrease in the threshold water-breaking radiation force with increasing beamwidth. This is consistent with the trend for the continuous wave (Figure 4.25) and pulsed wave case at 1 kHz (Figure 4.27).

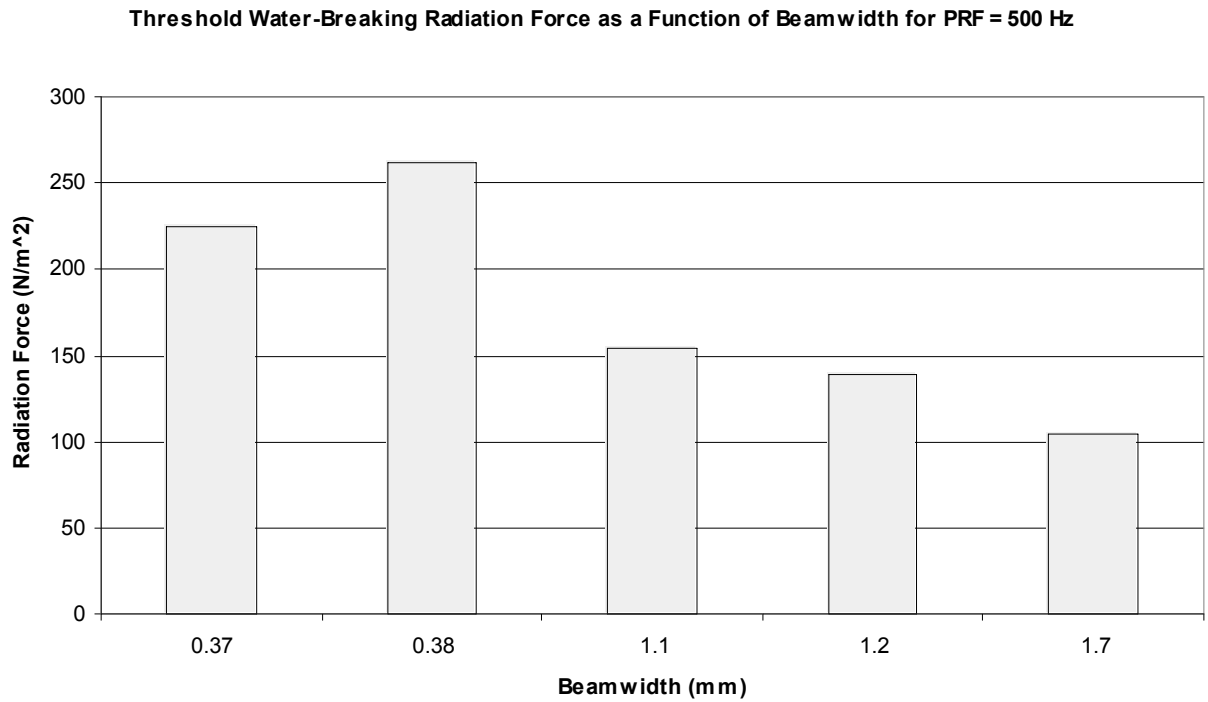


Figure 4.28 Threshold Water-Breaking Radiation Force due to Beamwidth for the PRF = 500 Hz Case

Figure 4.29 shows the threshold water-breaking radiation force for the two pulsed wave case plotted as a function of increasing beamwidth. The top regression line (PRF = 500 Hz) in Figure 4.29 has the equation $P = -109.755b + 281.089$. The r^2 value for the linear regression line for PRF = 500 Hz is 0.94. The lower regression line (PRF = 1 kHz) in the same figure has the equation $P = -85.116b + 311.006$. The r^2 value for the linear regression line for PRF = 1 kHz is 0.84. There is a statistically significant difference (p -value < 0.05) in the threshold water-breaking compressional pressure for both pulsed cases as a function of beamwidth.

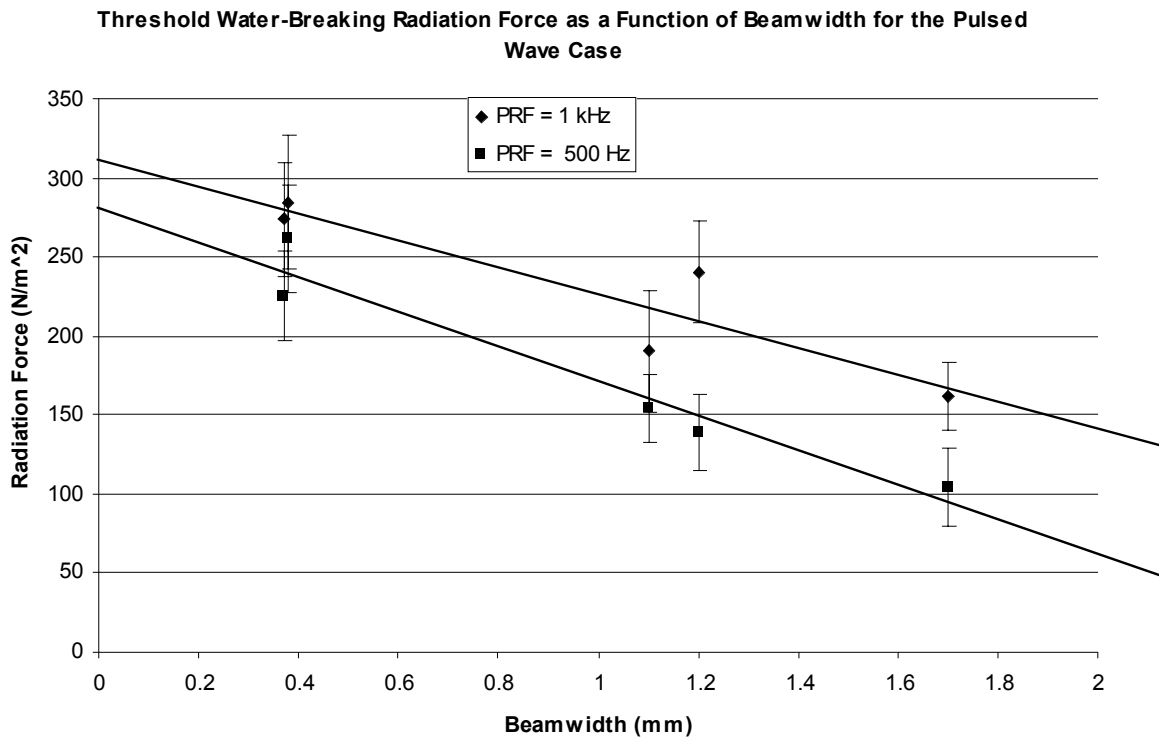


Figure 4.29 Threshold Water-Breaking Radiation Force for the Pulsed Wave Case with Beamwidth Dependency and a Linear Regression Line

In addition to determining how the pulse repetition frequency and beamwidth affect the threshold water-breaking radiation force, there has been interest in determining if the carrier frequency of the transducer affects the threshold water-breaking radiation force. Figure 4.30 shows how the threshold water-breaking radiation force varies as the carrier frequency varies. Each carrier frequency in Figure 4.30 is grouped into a set of three, where the first bar in each group represents the continuous wave condition, the second bar represents the higher pulsed wave condition, and the third bar represents the lower pulsed wave condition.

Radiation Force as a Function of Carrier Frequency

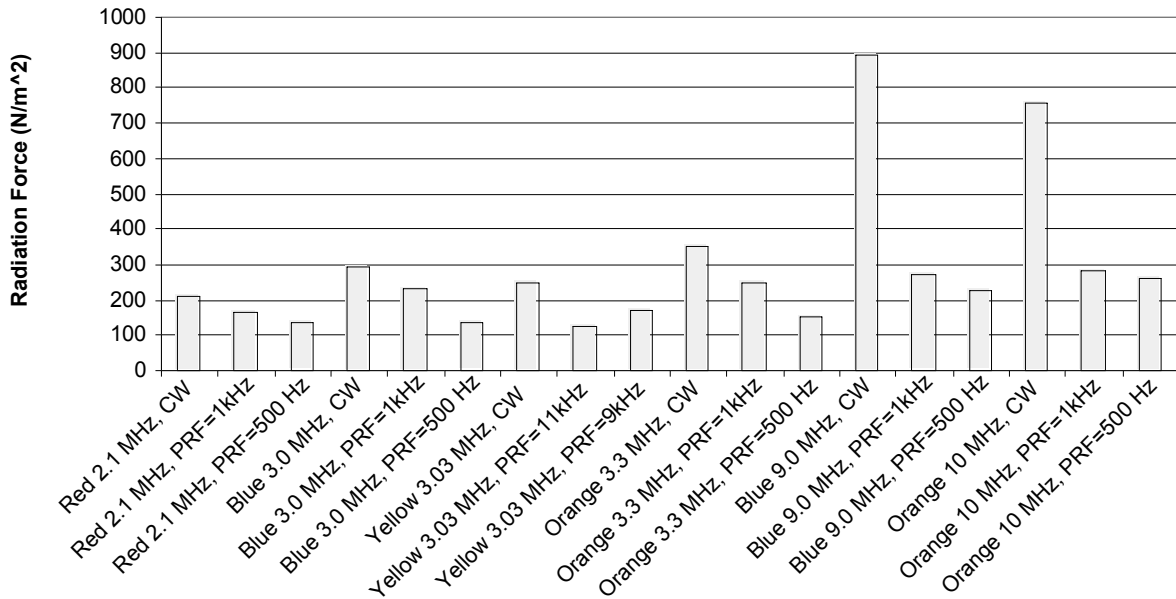


Figure 4.30 Threshold Water-Breaking Radiation Force due to Carrier Frequency

Figure 4.30 shows that there is no relationship between the carrier frequency and the threshold water-breaking radiation force. As the carrier frequency increases, the threshold water-breaking radiation force does not have an overall trend of changing to indicate frequency dependence. In addition, the blue, 3.0 MHz and yellow, 3.03 MHz transducers have center frequencies that are fairly close. However, the threshold water-breaking radiation forces for these two transducers for the continuous wave condition are not in the range of each other. The continuous wave threshold water-breaking radiation force for the blue, 3.0 MHz transducer is 292 N/m² and 247 N/m² for the yellow, 3.03 MHz transducer.

The effect ultrasonic frequency has on the threshold water-breaking radiation force can be seen in Figure 4.31-4.35. These figures show how the threshold water-breaking radiation force (y-axis) changes with a change in the frequency (x-axis). Figure 4.31 is the threshold water-breaking radiation force for the continuous wave case and Figure 4.33 is the threshold

water-breaking radiation force for the pulsed case, where the pulse repetition frequency is 1 kHz. Figure 4.34 is the threshold water-breaking radiation force for the pulsed case, where the pulse repetition frequency is 500 Hz.

Figure 4.31 (continuous wave case) shows that no trend in the threshold water-breaking radiation force can be observed as the frequency increases. However, at lower ultrasonic frequencies (2.1, 3, 3.03, and 3.3 MHz), the threshold water-breaking radiation force is less than that at higher ultrasonic frequencies (9 and 10 MHz).

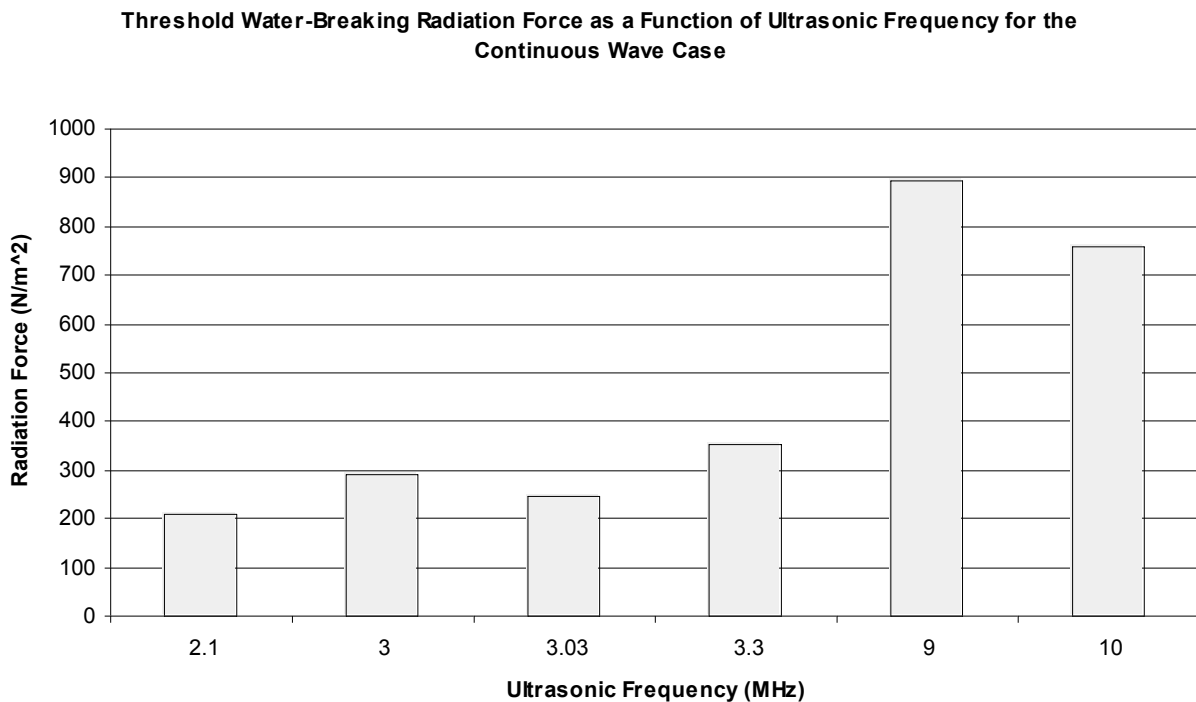


Figure 4.31 Threshold Water-Breaking Radiation Force due to Frequency for the Continuous Wave Case

Figure 4.32 shows the threshold water-breaking radiation force for the continuous wave case plotted as a function of increasing ultrasonic frequency. The regression line in Figure 4.32 has the equation $P = 081.276f + 46.626$. The r^2 value for the linear regression line is 0.94. There is a statistically significant difference (p -value < 0.05) in the threshold water-breaking radiation force as a function of the ultrasonic frequency.

Threshold Water-Breaking Rarefactional Pressure as Function of Ultrasonic Frequency for the Continuous Wave Case

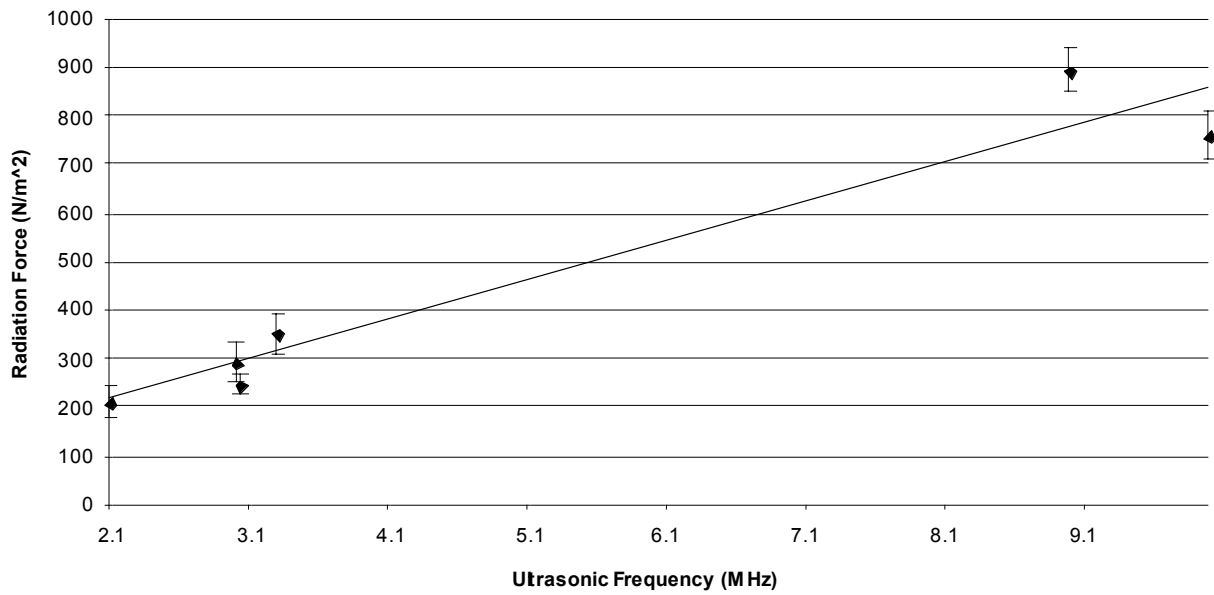


Figure 4.32 Threshold Water-Breaking Radiation Force for the Continuous Wave Case with Ultrasonic Frequency Dependency and a Linear Regression Line

Figure 4.33 (pulsed wave case, PRF = 1 kHz) shows that the threshold water-breaking radiation force increases as frequency increases. This is fairly consistent with the overall observation of the continuous wave case (Figure 4.31).

Threshold Water-Breaking Radiation Force as a Function of Ultrasonic Frequency for PRF = 1 kHz

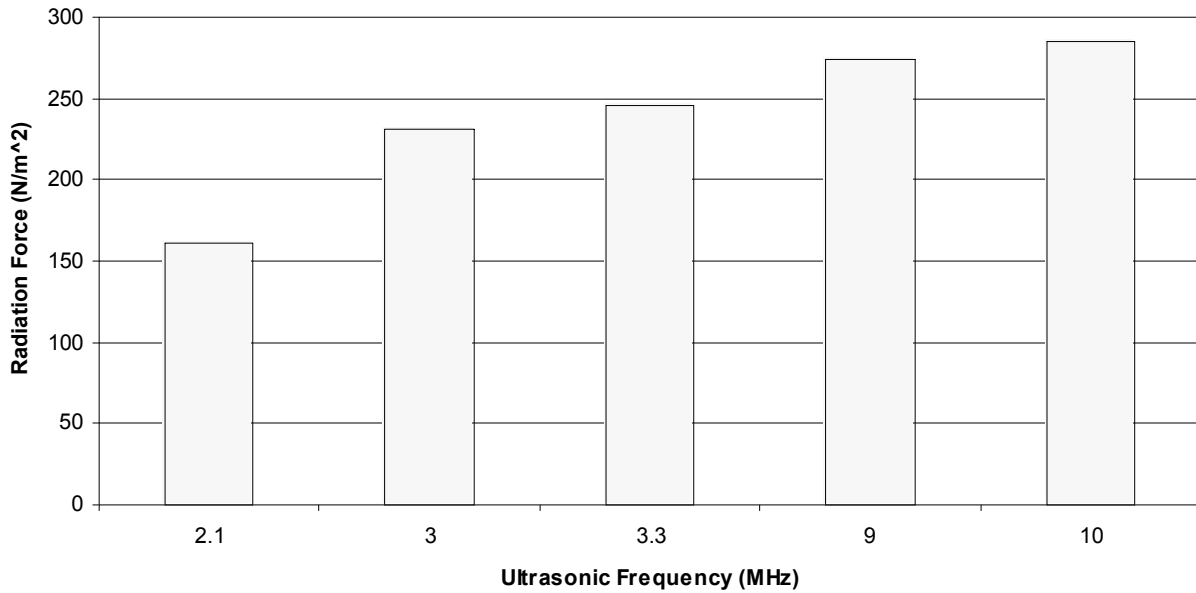


Figure 4.33 Threshold Water-Breaking Radiation Force due to Frequency for the PRF = 1 kHz

Figure 4.34 (pulsed wave case, PRF = 500 Hz) shows that the threshold water-breaking radiation force increases as frequency increases. This is fairly consistent with the overall observation of the continuous wave case (Figure 4.31) and the pulsed wave case at 1 kHz (Figure 4.33).

**Threshold Water-Breaking Radiation Force as a Function of Ultrasonic Frequency for
PRF = 500 Hz**

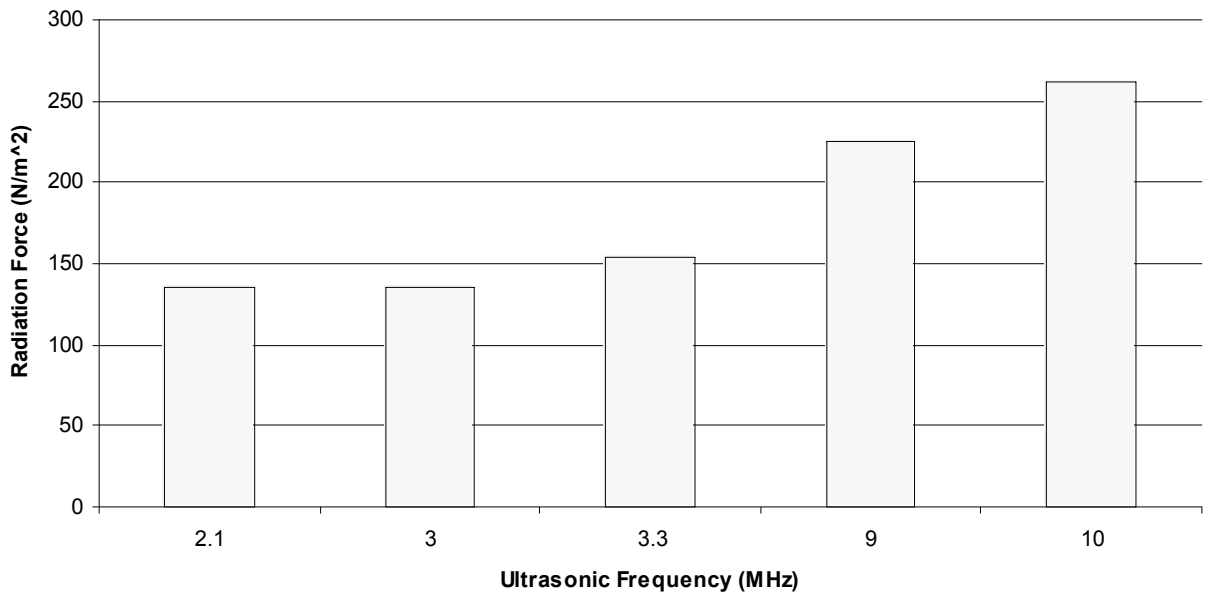


Figure 4.34 Threshold Water-Breaking Radiation Force due to Frequency for the PRF = 500 Hz

Figure 4.35 shows the threshold water-breaking radiation force for the two pulsed wave case plotted as a function of increasing ultrasonic frequency. The top regression line (PRF = 500 Hz) in Figure 4.35 has the equation $P = 17.075f + 83.249$. The r^2 value for the linear regression line for PRF = 500 Hz is 0.96. The lower regression line (PRF = 1 kHz) in the same figure has the equation $P = 12.581f + 161.201$. The r^2 value for the linear regression line for PRF = 1 kHz is 0.77. There is a statistically significant difference (p -value < 0.05) in the threshold water-breaking radiation force for the both pulsed cases as a function of ultrasonic frequency.

Threshold Water-Breaking Radiation Force as a Function of Ultrasonic Frequency for the Pulsed Wave Case

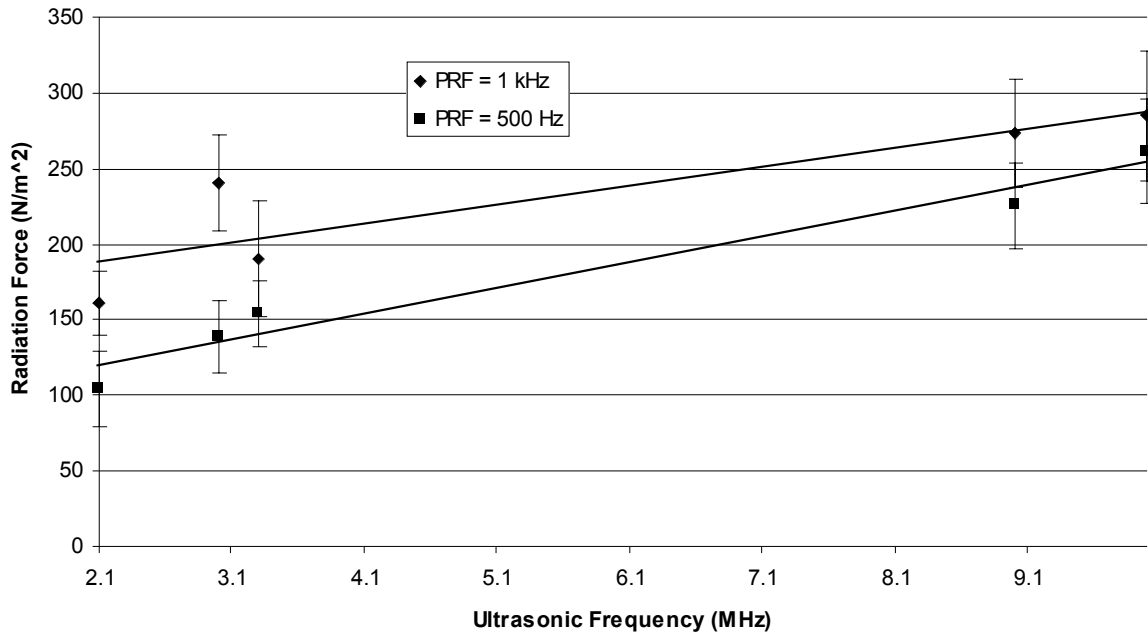


Figure 4.35 Threshold Water-Breaking Radiation Force for the Pulsed Wave Case with Ultrasonic Frequency Dependency and a Linear Regression Line

Figure 4.36 is a figure of how the threshold water-breaking force. Each carrier frequency in Figure 4.36 is grouped into a set of three, where the first bar in each group represents the continuous wave condition, the second bar represents the higher pulsed wave condition, and the third bar represents the lower pulsed wave condition. This figure is similar to Figure 4.29. However, the area of the beam is multiplied by the radiation force to obtain a force.

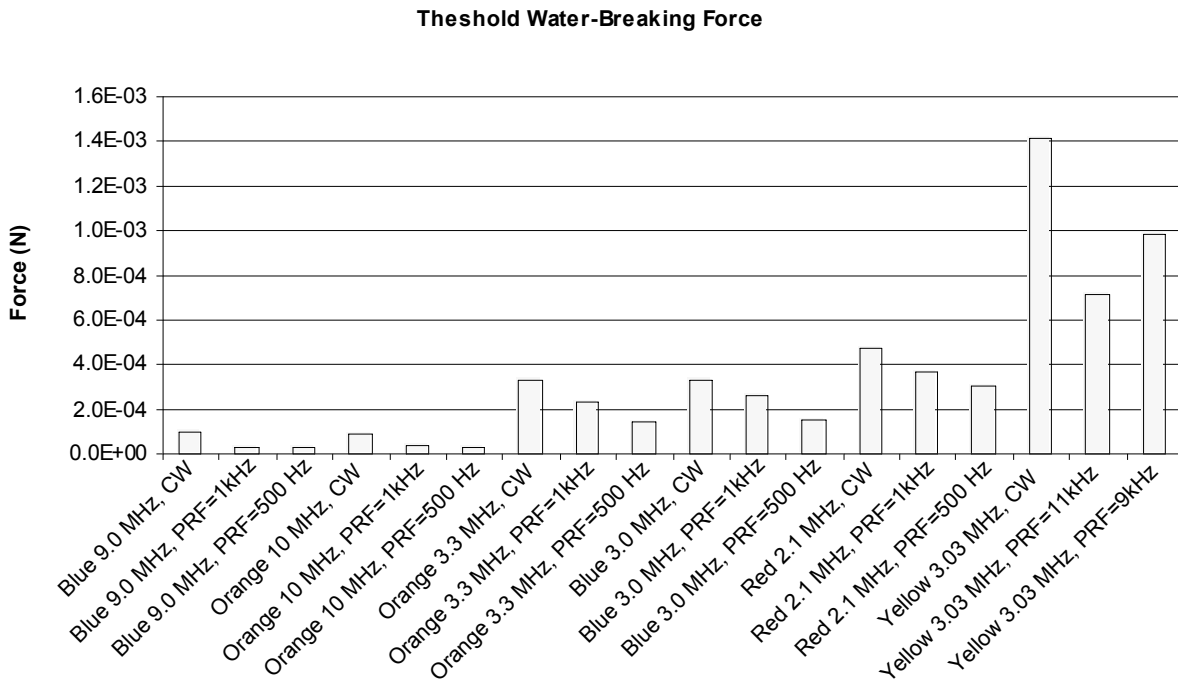


Figure 4.36 Threshold Water-Breaking Force